

PERFORMANCE OF A NEW CELLULAR CHANNEL ASSIGNMENT SCHEME INCLUDING HANDOFFS

by

GILBERT SHU WAI WONG

B.A.Sc. (Electronics Engineering), Simon Fraser University, 1996

A THESIS SUBMITTED IN PARTIAL FULFILLMENT OF

THE REQUIREMENTS FOR THE DEGREE OF

MASTER OF APPLIED SCIENCE

in

THE FACULTY OF GRADUATE STUDIES

DEPARTMENT OF ELECTRICAL AND COMPUTER ENGINEERING

We accept this thesis as conforming

to the required standard

THE UNIVERSITY OF BRITISH COLUMBIA

September 1998

© Gilbert Wong 1998

In presenting this thesis in partial fulfilment of the requirements for an advanced degree at the University of British Columbia, I agree that the Library shall make it freely available for reference and study. I further agree that permission for extensive copying of this thesis for scholarly purposes may be granted by the head of my department or by his or her representatives. It is understood that copying or publication of this thesis for financial gain shall not be allowed without my written permission.

Department of Electrical and Computer Engineering

The University of British Columbia

2075 Wesbrook Place

Vancouver, Canada

V6T 1W5

Date:

September 30, 1998

Abstract

As the demand for cellular communication services is increasing rapidly, it is important to achieve an efficient utilization of the allocated radio spectrum. To this end, a channel assignment scheme that is consistent with the objectives of increasing capacity and minimizing interference is required. In this thesis, a dynamic channel assignment (DCA) scheme with channel borrowing and re-assignment is proposed. With the channel borrowing and re-assigning strategy, a cell which has no channel available may borrow a channel from an available channel set of its neighboring cells. The performance of the proposed DCA scheme is studied through computer simulations in terms of blocking probabilities and handoff activities. A comparison of blocking probabilities between the proposed scheme and some existing channel assignment schemes is made. In the no handoff case, the proposed scheme can significantly improve the blocking probability of the cells that have a complete set of interfering cells. In the case with handoff, the adaptability of the channel borrowing and re-assigning strategy leads to a significant improvement in handoff blocking probability for both uniform and non-uniform traffic distributions. The proposed scheme also generally has a lower overall blocking probability.

Table of Contents

Abstract	ii
List of Figures	vi
Acknowledgment	x
Chapter 1 Introduction	1
1.1 Motivation and Objectives.....	2
1.2 Outline of the Thesis.....	2
Chapter 2 Background	4
2.1 Cellular System and Frequency Reuse	4
2.2 Review of Other Channel Assignment Schemes	7
2.2.1 Fixed Channel Assignment Scheme	8
2.2.2 Borrowing with Directional Locking Scheme	9
2.2.3 Compact Pattern Dynamic Channel Assignment Scheme.....	14
2.2.4 Dynamic Channel Assignment Scheme Using Cost Function.....	15
2.2.5 Dynamic Channel Assignment Scheme Using Hopfield Neural Network ...	18
Chapter 3 Description of the Proposed DCA Scheme	20
3.1 Proposed Dynamic Channel Assignment Scheme.....	21
3.1.1 Channel Allocation Algorithm.....	21
3.1.2 Channel Borrowing and Re-assigning Strategy	24
3.1.3 Channel De-allocation Algorithm.....	28
3.2 Summary.....	30
Chapter 4 Performance Results with No Handoff	31
4.1 Simulation Model	31

4.1.1	Cellular System Layout	31
4.1.2	Call Arrival and Call Duration Models.....	33
4.1.3	Performance Measures for Channel Assignment Schemes	34
4.2	Operational Parameters for Channel Allocation and De-allocation	35
4.2.1	Nominal Channel Condition	35
4.2.2	Resonance Condition	37
4.3	Results and Discussions.....	40
4.3.1	Uniform Traffic Distribution	41
4.3.2	Call Blocking Distribution.....	44
4.3.3	Non-uniform Traffic Distribution	46
4.4	Summary	48
Chapter 5	Performance Results with Handoff	49
5.1	Mobility Models	50
5.2	Handoff Model.....	52
5.3	FCA Blocking Probability with Mobility Model A and B	52
5.4	Results and Discussions.....	61
5.4.1	Uniform Traffic Distribution	61
5.4.2	Call Blocking Distribution.....	71
5.4.3	Non-uniform Traffic Distribution	74
5.5	Summary	78
Chapter 6	Conclusion	79
6.1	Future Works	80
Glossary		81

Bibliography**83**

List of Figures

Figure 2.1:	Structure of a Cellular System.	4
Figure 2.2:	Co-channel Interference from Six Interfering BS's.	6
Figure 2.3:	Channel Borrowing and Co-channel Cell Locking.	10
Figure 2.4:	Examples Illustrating Channel Re-allocation Scheme.	12
Figure 2.5:	Channel Re-allocation of the BDCL Scheme.	13
Figure 2.6:	Compact Allocation Patterns: (a) Clockwise Pattern, (b) Anticlockwise Pattern.	14
Figure 3.1:	Channel Allocation with Channel Borrowing and Re-assigning Strategy.	23
Figure 3.2:	Channel Borrowing and Re-assigning Strategy: (a) Borrow from the First Tier Cell, (b) Borrow from the Second Tier Cell.	26
Figure 3.3:	Channel Borrowing and Re-assigning Strategy.	27
Figure 3.4:	Channel De-allocation Algorithm.	29
Figure 4.1:	Cellular System for Simulation of the Proposed DCA Scheme.	32
Figure 4.2:	Simulation Results of New Call Blocking Probability, P_{bn} , (averaged over central 9 cells) for the Proposed DCA Scheme with (i) $\alpha = 0$, (ii) $\alpha = 1$, and (iii) $\alpha = 2$	36
Figure 4.3:	Simulation Results of New Call Blocking Probability, P_{bn} , (averaged over 49 cells) for the Proposed DCA Scheme with (i) $\alpha = 0$, (ii) $\alpha = 1$, and (iii) $\alpha = 2$	37
Figure 4.4:	Simulation Results of New Call Blocking Probability, P_{bn} , (averaged over central 9 cells) for the Proposed DCA Scheme with (i) $\beta = 0$, (ii) $\beta = 1$, (iii) $\beta = 3$, and (iv) $\beta = 4$	39
Figure 4.5:	Simulation Results of New Call Blocking Probability, P_{bn} , (averaged over 49 cells) for the Proposed DCA Scheme with (i) $\beta = 0$, (ii) $\beta = 1$, (iii) $\beta = 3$, and (iv) $\beta = 4$	39
Figure 4.6:	New Call Blocking Probability, P_{bn} , (averaged over central 9 cells) with Uniform Traffic Distribution.	41
Figure 4.7:	New Call Blocking Probability, P_{bn} , (averaged over 49 cells) with Uniform Traffic Distribution.	43

Figure 4.8:	Parallelogram-shaped Cellular Network with Three Tiers.	44
Figure 4.9:	Total Call Blocking Probability, P_b , for Three Different Tier Cells with Uniform Traffic Distribution.	45
Figure 4.10:	Non-uniform Traffic Distribution (calls/hour) in a 49-Cell System: (a) Traffic Distribution Pattern A, (b) Traffic Distribution Pattern B.	46
Figure 4.11:	New Call Blocking Probability, P_{bn} , (averaged over 49 cells) with Non-uniform Traffic Distribution Pattern A.	47
Figure 4.12:	New Call Blocking Probability, P_{bn} , (averaged over 49 cells) with Non-uniform Traffic Distribution Pattern B.	47
Figure 5.1:	Mobile Motion Examples: (a) Mobility Model A, (b) Mobility Model B.	51
Figure 5.2:	Markov Chain State Diagram for FCA Scheme.	53
Figure 5.3:	Approximation of Handoff Arrival Rate λ_h and Blocking Probability of Call Channel Requests P_b'	55
Figure 5.4:	Average Number of Handoffs per Successful Call as a Function of MS Maximum Speed with Mobility Model A.	56
Figure 5.5:	Average Number of Handoffs per Successful Call as a Function of MS Maximum Speed with Mobility Model B.	57
Figure 5.6:	Approximate and Simulation Results for Total Call Blocking Probability, P_b , for the FCA Scheme (averaged over 49 cells) with Mobility Model A. (a) $V_{\max} = 20$ km/hr, (b) $V_{\max} = 40$ km/hr, (c) $V_{\max} = 60$ km/hr, (d) $V_{\max} = 80$ km/hr, (e) $V_{\max} = 100$ km/hr, (f) $V_{\max} = 120$ km/hr.	59
Figure 5.7:	Approximate and Simulation Results for Total Call Blocking Probability, P_b , for the FCA Scheme (averaged over 49 cells) with Mobility Model B. (a) $V_{\max} = 20$ km/hr, (b) $V_{\max} = 40$ km/hr, (c) $V_{\max} = 60$ km/hr, (d) $V_{\max} = 80$ km/hr, (e) $V_{\max} = 100$ km/hr, (f) $V_{\max} = 120$ km/hr.	60
Figure 5.8:	New Call Blocking Probability, P_{bn} , (averaged over central 9 cells) with Mobility Model A. (a) $V_{\max} = 60$ km/hr, (b) $V_{\max} = 120$ km/hr.	62
Figure 5.9:	Handoff Blocking Probability, P_{bh} , (averaged over central 9 cells) with Mobility Model A. (a) $V_{\max} = 60$ km/hr, (b) $V_{\max} = 120$ km/hr.	62
Figure 5.10:	Dropped Call Probability, P_{dc} , (averaged over central 9 cells) with Mobility Model A. (a) $V_{\max} = 60$ km/hr, (b) $V_{\max} = 120$ km/hr.	63

Figure 5.11:	Total Call Blocking Probability, P_b , (averaged over central 9 cells) with Mobility Model A. (a) $V_{\max} = 60$ km/hr, (b) $V_{\max} = 120$ km/hr.	63
Figure 5.12:	New Call Blocking Probability, P_{bn} , (averaged over 49 cells) with Mobility Model A. (a) $V_{\max} = 60$ km/hr, (b) $V_{\max} = 120$ km/hr.	64
Figure 5.13:	Handoff Blocking Probability, P_{bh} , (averaged over 49 cells) with Mobility Model A. (a) $V_{\max} = 60$ km/hr, (b) $V_{\max} = 120$ km/hr.	64
Figure 5.14:	Dropped Call Probability, P_{dc} , (averaged over 49 cells) with Mobility Model A. (a) $V_{\max} = 60$ km/hr, (b) $V_{\max} = 120$ km/hr.	65
Figure 5.15:	Total Call Blocking Probability, P_b , (averaged over 49 cells) with Mobility Model A. (a) $V_{\max} = 60$ km/hr, (b) $V_{\max} = 120$ km/hr.	65
Figure 5.16:	New Call Blocking Probability, P_{bn} , (averaged over central 9 cells) with Mobility Model B. (a) $V_{\max} = 60$ km/hr, (b) $V_{\max} = 120$ km/hr.	67
Figure 5.17:	Handoff Blocking Probability, P_{bh} , (averaged over central 9 cells) with Mobility Model B. (a) $V_{\max} = 60$ km/hr, (b) $V_{\max} = 120$ km/hr.	67
Figure 5.18:	Dropped Call Probability, P_{dc} , (averaged over central 9 cells) with Mobility Model B. (a) $V_{\max} = 60$ km/hr, (b) $V_{\max} = 120$ km/hr.	68
Figure 5.19:	Total Call Blocking Probability, P_b , (averaged over central 9 cells) with Mobility Model B. (a) $V_{\max} = 60$ km/hr, (b) $V_{\max} = 120$ km/hr.	68
Figure 5.20:	New Call Blocking Probability, P_{bn} , (averaged over 49 cells) with Mobility Model B. (a) $V_{\max} = 60$ km/hr, (b) $V_{\max} = 120$ km/hr.	69
Figure 5.21:	Handoff Blocking Probability, P_{bh} , (averaged over 49 cells) with Mobility Model B. (a) $V_{\max} = 60$ km/hr, (b) $V_{\max} = 120$ km/hr.	69
Figure 5.22:	Dropped Call Probability, P_{dc} , (averaged over 49 cells) with Mobility Model B. (a) $V_{\max} = 60$ km/hr, (b) $V_{\max} = 120$ km/hr.	70
Figure 5.23:	Total Call Blocking Probability, P_b , (average over 49 cells) with Mobility Model B. (a) $V_{\max} = 60$ km/hr, (b) $V_{\max} = 120$ km/hr.	70
Figure 5.24:	New Call Blocking Probability, P_{bn} , of Three Tier Cells for the Proposed DCA Scheme with Mobility Model A and Three Different MS Maximum Speeds ($V_{\max} = 20, 60$, and 120 km/hr).	72
Figure 5.25:	Handoff Blocking Probability, P_{bh} , of Three Tier Cells for the Proposed DCA Scheme with Mobility Model A and Three Different MS Maximum Speeds ($V_{\max} = 20, 60$, and 120 km/hr).	73

Figure 5.26:	Total Call Blocking Probability, P_b , of Three Tier Cells for the Proposed DCA Scheme with Mobility Model A and Three Different MS Maximum Speeds ($V_{\max} = 20, 60$, and 120 km/hr).	73
Figure 5.27:	New Call Blocking Probability, P_{bn} , (averaged over 49 cells) with Mobility Model A ($V_{\max} = 60$ km/hr) and Non-uniform Traffic Distribution Pattern A.	75
Figure 5.28:	New Call Blocking Probability, P_{bn} , (averaged over 49 cells) with Mobility Model B ($V_{\max} = 60$ km/hr) and Non-uniform Traffic Distribution Pattern A.	75
Figure 5.29:	Handoff Blocking Probability, P_{bh} , (averaged over 49 cells) with Mobility Model A ($V_{\max} = 60$ km/hr) and Non-uniform Traffic Distribution Pattern A.	76
Figure 5.30:	Handoff Blocking Probability, P_{bh} , (averaged over 49 cells) with Mobility Model B ($V_{\max} = 60$ km/hr) and Non-uniform Traffic Distribution Pattern A.	76
Figure 5.31:	Total Call Blocking Probability, P_b , (averaged over 49 cells) with Mobility Model A ($V_{\max} = 60$ km/hr) and Non-uniform Traffic Distribution Pattern A.	77
Figure 5.32:	Total Call Blocking Probability, P_b , (averaged over 49 cells) with Mobility Model B ($V_{\max} = 60$ km/hr) and Non-uniform Traffic Distribution Pattern A.	77

Acknowledgment

I would like to thank my Lord Almighty for His love, His grace, and His blessings. I would like to thank my supervisor, Dr. Cyril Leung, for his excellent supervision, patience, and encouragement throughout the research project. Without his precious suggestions and time, this thesis would have never been finished. Also, I would like to thank Raymond Kwan and Johnson Sebeni for helpful discussions with me. In addition, I would like to express my sincerest gratitude to my parents, my brother, and my sister for their support and care.

Last but not least, I would like to thank Cony Chan for her love and encouragement in the past two years. Because of her love and encouragement, the completion of this thesis becomes possible.

Chapter 1 Introduction

The rapid development of wireless communication technologies in the last decade has led to a significant increase in the demand for mobile telephones, especially in the developed countries. The present cellular mobile telephone systems serve a large number of users over a vast geographical area [1, 2]. The continuous advances in wireless communication technologies have also improved the quality and reliability of various cellular networks. People in different locations and countries are able to communicate with one another through the cellular networks by using their handheld mobile telephones. In addition, improvements in mobile communication technology have reduced the cost of providing cellular telephone services. As a result, the cellular mobile industry has experienced a tremendous growth. Nevertheless, the available radio frequency spectrum of cellular systems is a limited resource. To accommodate the growth of mobile users and maintain a reliable service, it is necessary to develop efficient frequency spectrum utilization schemes. A channel assignment scheme which is consistent with the objectives of increasing capacity and minimizing interference is required.

A basic cellular system consists of mobile stations (MS), base stations (BS), and a mobile switching center (MSC) [1, 2]. The BS is responsible for providing a wireless connection between the MS and the public switched telephone network (PSTN). When a cellular mobile telephone is turned on, it first scans a group of control channels and chooses one with the strongest signal. The strongest control channel indicates which cell is to serve the mobile-originating calls. The MS may initiate a call in the cellular network after selecting the control channel. The MS and the BS must scan all the available voice channels in order to find an unoccupied one to use. The process used by the MSC to assign a voice channel to the MS is called a channel assignment scheme. A

call may be blocked when the MSC is unable to allocate a voice channel to the MS. A handoff operation is performed when the MS moves from one cell to another while a call is in progress. In the handoff operation, the MSC transfers the call to a new channel available to the new BS. When the MS terminates a call or is handed off from one cell to its neighboring cell, the BS will update the status of each available voice channel.

1.1 Motivation and Objectives

To lower the blocking probability and provide high quality service in heavily loaded cellular communication systems, an efficient channel assignment scheme must be used. Such a channel assignment scheme reuses a voice channel (subject to interference constraints) in order to maximize the frequency spectrum utilization. It also lowers the probability of blocked calls and enhances the traffic-carrying capacity of cellular systems.

The objective of this thesis is to develop a dynamic channel assignment (DCA) scheme and to compare its performance with some existing schemes. The DCA scheme uses a simple cost function to assign a channel to a cell. The performance of the proposed DCA scheme when handoffs are considered is also examined in this thesis.

1.2 Outline of the Thesis

In Chapter 2, a number of different channel assignment schemes are reviewed. In Chapter 3, the proposed DCA scheme with channel borrowing and re-assigning strategy is

described. In Chapter 4, we examine the proposed scheme with no handoffs through computer simulations and compare its performance with those of different channel assignment schemes in terms of blocking probabilities for both uniform and non-uniform traffic distributions. The mobility model used and the performance of the proposed DCA scheme with handoffs are presented in Chapter 5. The conclusion and possible future studies are summarized in Chapter 6.

Chapter 2 Background

In this chapter, we first look at cell layouts and frequency reuse in a cellular mobile communication system. Several channel assignment strategies are then reviewed.

2.1 Cellular System and Frequency Reuse

In a cellular system, the service area is divided into a number of cells where each cell is served by an BS. The size of the cell depends on the transmission power of the BS transmitter. Every MS in the cell communicates with the BS via a channel in order to establish a wireless connection. The cellular system allocates a group of channels to each BS to serve the MS's within the cell. To simplify the design of the cellular system, each cell is assumed to have an identical size and hexagonal shape as shown in Figure 2.1.

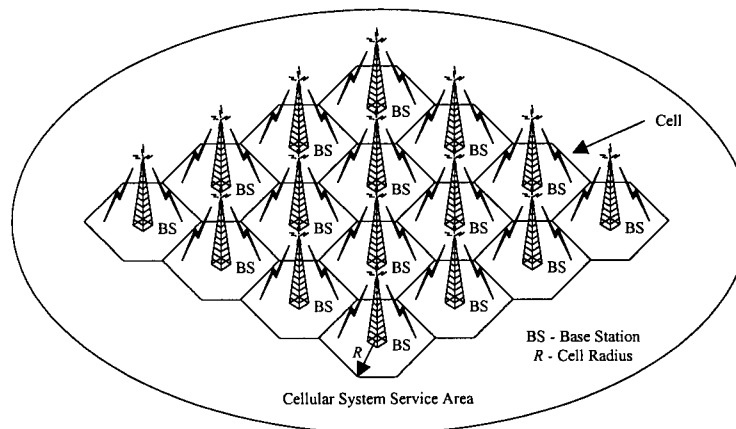


Figure 2.1: Structure of a Cellular System.

Because the frequency spectrum of wireless communications is a limited resource,

frequency reuse is the central concept in the cellular structure. Frequency reuse enables two MS's to use the same frequency channel simultaneously in different geographical regions without violating interference constraints. Thus, the frequency reuse plan directly affects the efficiency of frequency spectrum utilization in the cellular system.

The interference caused by frequency reuse is called co-channel interference and is usually the most important factor which determines the overall capacity of the cellular system. Frequency reuse makes use of radio propagation path losses provide an acceptable carrier-to-interference ratio (CIR). Cell separation is one effective way to reduce the co-channel interference. Assume that each BS has signal coverage in a cell of radius R (see Figure 2.1) and that the distance between the two nearest co-channel cell centers is D . The co-channel interference reduction factor (CIRF), a , [3] is defined as

$$a = \frac{D}{R}. \quad (2.1)$$

In (2.1), the value a is independent of the BS transmitted power and can be determined for any required CIR level [1]. As long as the BS transmit powers are the same in all the cells, an increase in the transmitted power equally in each cell does not increase co-channel interference. Because each cell is assumed to have an identical size, the required level of carrier to interference ratio can be determined by a function of R and D . The worst situation occurs when an MS is at the edge (boundary) of the cell. The received power at the MS from the BS is proportional to $R^{-\gamma}$ where the parameter γ is the path loss exponent and its value varies between 2 and 4. Furthermore, the received power at the MS due to the i th interfering cell is proportional to $D_i^{-\gamma}$ where D_i is the distance between the MS and the i th interferer. Figure 2.2 shows the interference from the six

nearest co-channel cells.

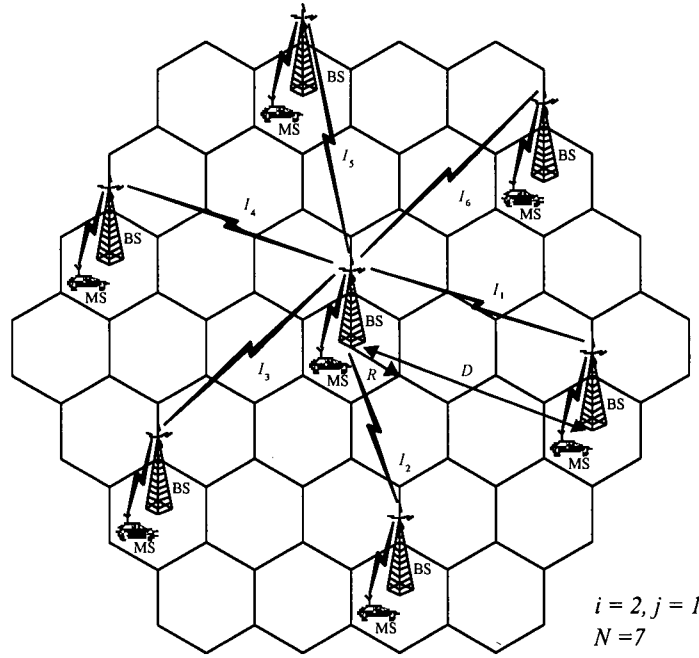


Figure 2.2: Co-channel Interference from Six Interfering BS's.

To simplify the calculation, we assume that the interfering BS's are equidistant from the desired BS and that the distance between the two nearest co-channel BS's is D (See Figure 2.2).

The CIR of the MS is then approximately given by

$$\frac{C}{I} = \frac{R^{-\gamma}}{\sum_{i=1}^6 (D_i)^{-\gamma}} = \frac{R^{-\gamma}}{6D^{-\gamma}} = \frac{a^{\gamma}}{6}. \quad (2.2)$$

To provide an acceptable CIR level, the minimum distance D can be obtained from (2.2).

For the hexagonal cell structure, the relationship between the CIRF and the frequency reuse factor, N , is given by [2]

$$\frac{D}{R} = \sqrt{3N}. \quad (2.3)$$

To tessellate the hexagonal-shaped cellular system without gaps between adjacent cells, the frequency reuse factor must satisfy

$$N = i^2 + ij + j^2 \quad (2.4)$$

where the parameters i and j are non-negative integers.

2.2 Review of Other Channel Assignment Schemes

A number of channel assignment schemes appear in [4-12]. The objective of a channel assignment scheme is to minimize the co-channel interference and increase frequency spectrum utilization in a cellular system. Channel assignment schemes can be classified as either fixed or dynamic. In a fixed channel assignment (FCA) scheme, a predetermined set of channels are allocated to each cell. A dynamic channel assignment (DCA) scheme places all channels in a central pool and assigns a channel to a new call while ensuring that co-channel interference constraints are not violated [4]. Because of its flexibility and traffic adaptability, DCA may increase the trunking capacity of the cellular system and reduce the probability of blocked calls. The trunking capacity exploits the statistical behavior of users so that a fixed number of channels may serve a large, random user population [2].

2.2.1 Fixed Channel Assignment Scheme

A FCA scheme allocates a predetermined set of channels to each cell permanently and a channel used in a cell must satisfy co-channel reuse constraints [1]. The total number, M , of available channels in the cellular system is divided into a number of nominal channel sets. Each nominal channel set consists of S channels with

$$S = \frac{M}{N} \quad (2.5)$$

where the frequency reuse factor N is defined in (2.4). In the FCA scheme, the frequency reuse scheme allocates the same set of S channels to cells separated by at least a distance D . Because each cell has the same number of nominal channels, this uniform channel distribution is the most efficient when the cellular system also has a uniform traffic distribution. The overall average blocking probability of the cellular system is the same as the probability of a blocked call in each cell. The blocking probability for the FCA scheme can be obtained using the Erlang B formula [2]

$$P_b = \frac{\left(\frac{\lambda_t}{\mu_t}\right)^S}{S! \sum_{n=0}^S \frac{\lambda_t^n}{n! \mu_t^n}} \quad (2.6)$$

In (2.6), λ_t is the mean call arrival rate due to new calls and handoffs while μ_t is the mean call departure rate due to terminations from call completions and handoffs. The Erlang B formula is based upon the following assumptions:

- New call arrivals and handoff call arrivals form a Poisson process with mean call arrival rates of λ_n and λ_h respectively.

- The call duration is exponentially distributed with an expected value of T_m and the mean outgoing handoff rate per calling mobile is μ_h .

However, the traffic distribution of the cellular system may be non-uniform due to the user distribution and terrain environment of the service area. As a result, one cell may under-utilize its available channels while an adjacent cell may have a high call blocking probability. The FCA scheme may result in poor channel utilization when the traffic distribution is non-uniform. Although the FCA scheme is very simple, it does not adapt to changing traffic conditions and user distribution. In order to improve the performance of channel assignment in the non-uniform traffic system, channel borrowing schemes have been proposed.

2.2.2 Borrowing with Directional Locking Scheme

In the simple borrowing (SB) scheme [5], a group of nominal channels is allocated to each cell. Channel borrowing scheme [5-7] are a form of DCA which only needs local and neighboring cell information. Unlike the FCA scheme, when all nominal channels of the cell are busy, an available nominal channel from the adjacent cell is borrowed to serve a call. The borrowed nominal channel must not interfere with existing calls. If no such channel can be borrowed, the call is blocked.

In Figure 2.3, cell x borrows channel i from cell y_1 . This causes channel i to be locked¹ in cells y_2 and y_3 which are co-channel cells of y_1 . The selection rule for the borrowed channel

¹ A channel is locked in cell x if use of the channel in cell x will cause a violation of co-channel interference constraints.

plays an important role in the channel borrowing strategy because the set of borrowable channels in a cell may have more than one available channel. To minimize the blocking probability of future calls, the rule for selecting a borrowable channel is to generally borrow from an adjacent cell having the largest available channel set. An efficient channel borrowing strategy must reduce the number of locked channels in order to increase the channel utilization and decrease the call blocking probability.

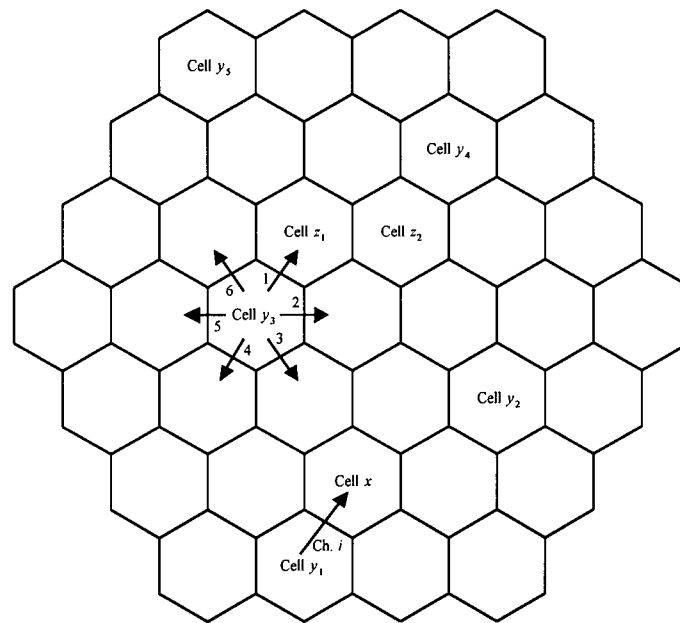


Figure 2.3: Channel Borrowing and Co-channel Cell Locking.

The borrowing with channel ordering (BCO) scheme [6] is introduced to provide an efficient method of selecting the borrowable channel. In the BCO scheme, all nominal channels in each cell are numbered $1, 2, \dots, S$. The lowest-number available channel in the nominal channel set has the highest priority to be assigned to the next local call while the highest-number available nominal channel is given the highest priority to be borrowed temporarily by neighboring cells. The borrowed channel is not only selected from an adjacent cell having the largest available

channel set; it is also chosen to have the highest-number available channel of the neighboring cell. To minimize channel borrowing of future calls and the number of locked channels, the channel re-allocation scheme is used to reduce the traffic carried on borrowed channels. When a call is terminated, a channel is re-allocated in accordance with the following rules. Figure 2.4 illustrates some channel re-allocation examples for the BCO scheme.

- Assume that there are six calls in cell x served by nominal channels 1, 2, ..., 6. When the call served by channel 4 is terminated, the call served by channel 6 is switched to channel 4 and channel 6 is released. See Figure 2.4(a).
- Assume that there are twelve calls in cell x served by nominal channels 1, 2, ..., 10 and borrowed channels 19 and 20 from cell y_1 . When the call served by channel 6 is terminated, the call served by borrowed channel 19 is switched to channel 6 and borrowed channel 19 is released and un-locked in the three interfering cells (y_1, y_2, y_3) . See Figure 2.4(b).
- Assume that there are twelve calls in cell x served by nominal channels 1, 2, ..., 10 and borrowed channels 19 and 20 from cell y_1 . When the call served by borrowed channel 20 is terminated, the call served by borrowed channel 19 is switched to channel 20 and borrowed channel 19 is released and un-locked in the three interfering cells (y_1, y_2, y_3) . See Figure 2.4(c).

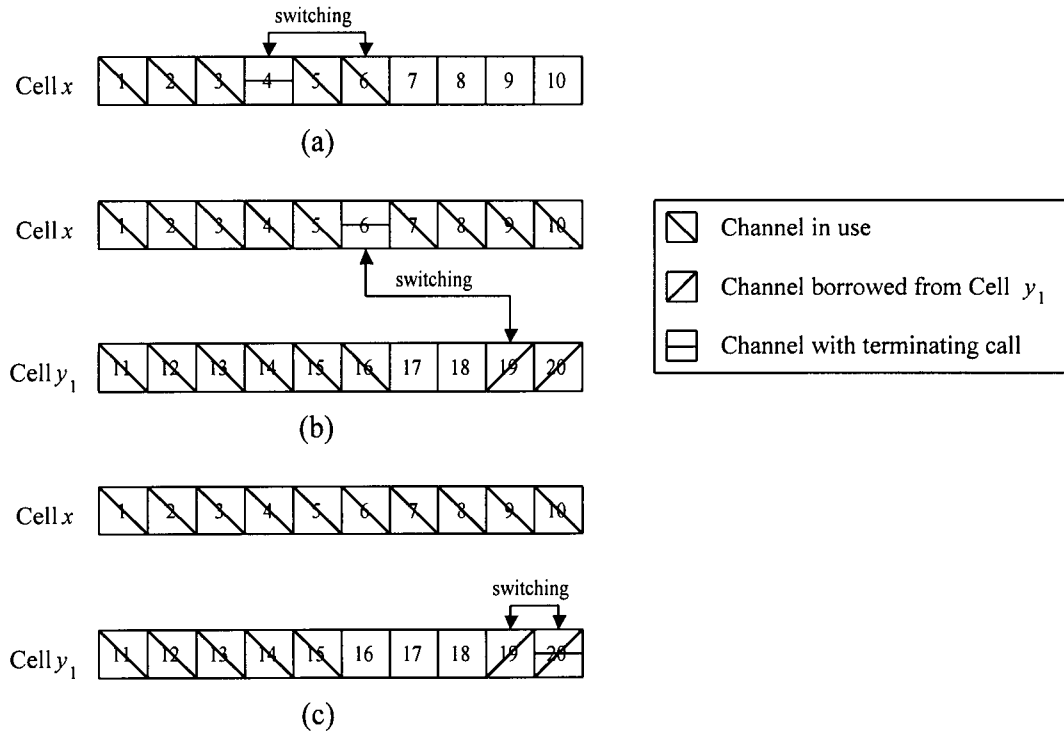


Figure 2.4: Examples Illustrating Channel Re-allocation Scheme.

In the BCO scheme, cell x is only allowed to borrow a channel from its neighboring cell y_1 where the borrowed channel is simultaneously free in three nearby co-channel cells (y_1, y_2, y_3). This severe requirement may increase the number of locked channels so that the number of available channels for the channel borrowing strategy is reduced. The borrowing with directional channel locking (BDCL) scheme [7] was developed to improve the availability of borrowable channels.

The BDCL scheme only locks a borrowed channel in co-channel cells where the borrowed channel used in those cells may cause a violation of co-channel interference constraints. In Figure 2.3, cell x borrows channel i from cell y_1 so that this causes channel i to be locked in cells

y_2 and y_3 which are co-channel cells of y_1 . Unlike the BCO scheme, channel i in cell y_3 only needs to be locked in directions 2, 3, and 4. Cells in directions 1, 5, and 6 are allowed to borrow channel i from cell y_3 without interfering the call served by channel i in cell x . Because cell z_1 is in direction 1 of cell y_3 , it can borrow channel i whether the locking conditions in cells y_4 and y_5 are satisfied. The BDCL scheme specifies the “lock directions” for each locked channel in order to determine the availability of borrowable “locked” channels. Therefore, the number of available channels for borrowing is greater than in the BCO scheme because a cell can lend a channel to a neighboring cell if co-channel interference constraints are not violated.

The BDCL scheme adopts the channel re-allocation scheme of calls from borrowed to nominal channels and between borrowed channels to minimize channel borrowing of future calls (See Figure 2.4). In Figure 2.5, the call served by borrowed channel 19 is switched to channel 6 when channel 6 in cell x is completely unlocked (i.e., unlocked in all 6 directions). The re-allocation rule shown in Figure 2.5 can reduce the amount of multiple channel borrowings.

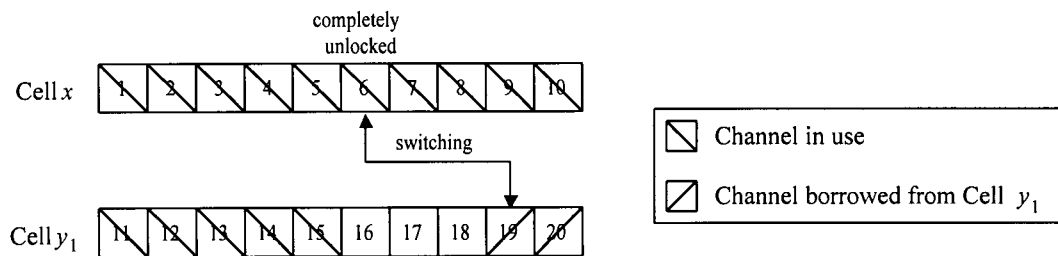


Figure 2.5: Channel Re-allocation of the BDCL Scheme.

2.2.3 Compact Pattern Dynamic Channel Assignment Scheme

A compact pattern based dynamic channel assignment scheme called CP-based DCA (CP-DCA) is described in [8]. The objective of the CP-DCA scheme is to maintain the co-channel cells of any channel to a compact pattern in a cellular system. The compact pattern is defined as the channel allocation pattern with the minimum average distance between two co-channel cells [9]. Figure 2.6 shows two compact allocation patterns (clockwise and anticlockwise patterns) where the minimum co-channel reuse distance is three cell units. With the center cell moved to one of the six neighboring cells, there are six other possible compact patterns. Therefore, the total number of compact patterns is $2 \times 7 = 14$.

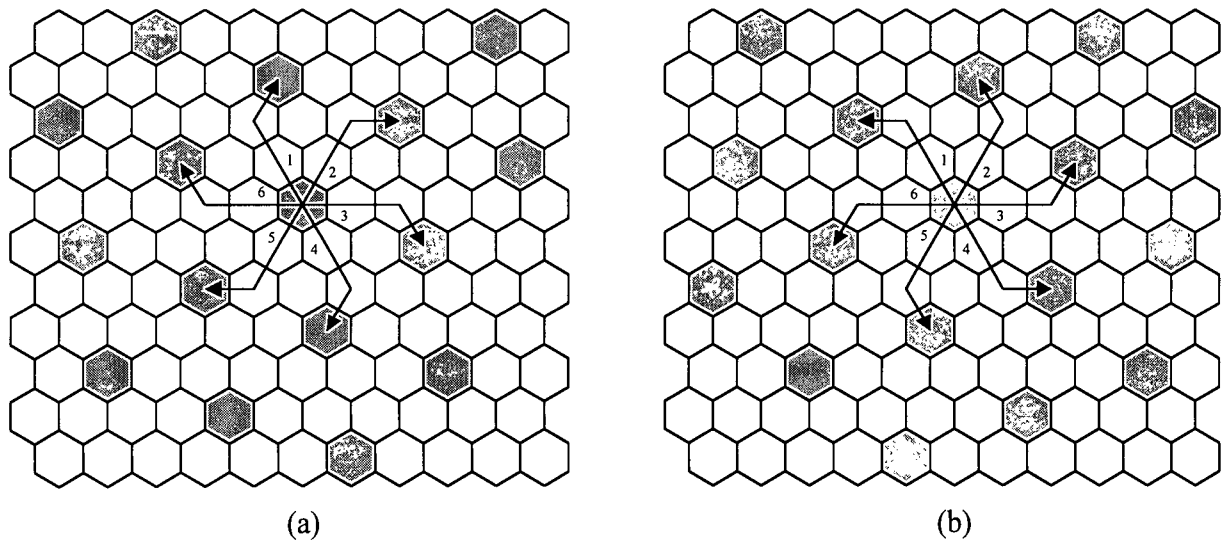


Figure 2.6: Compact Allocation Patterns: (a) Clockwise Pattern, (b) Anticlockwise Pattern.

The CP-DCA scheme consists of two phases: channel allocation and channel packing. Channel allocation assigns an unused channel to a new call while channel packing restores the compact pattern of the cellular system. Channel packing is only performed when the compact

channel is released. The compact channel is a channel which is allocated in accordance with any one of the fourteen compact patterns. The CP-DCA scheme shows that the number of channel re-assignment per released call in the channel packing phase is at most one [9].

2.2.4 Dynamic Channel Assignment Scheme Using Cost Function

In [10], a DCA scheme is described which uses a cost function. It allows any one of the M channels to be used in any cell in the cellular network to achieve an efficient frequency spectrum utilization. The cost function is used to evaluate the cost of using each of the available channels. The DCA scheme in [10] is distributed because the available and used channel lists are updated by exchanging status information between BS's whenever a new call arrives or a call is terminated.

This DCA scheme consists of two phases: channel allocation and channel de-allocation. A cost function is applied in the channel allocation to assign an unused channel to a new call from the available channel set $\Lambda(x)$ of cell x . The goal of the channel de-allocation phase is used to release a channel from the used channel set $A(x)$ which becomes available in the greatest number of interfering cells, $I(x)$. Initially, the DCA scheme allocates a set of nominal channels $F_D(x)$ to each cell x . Each nominal channel set contains S channels as in (2.5). With this nominal channel condition, the DCA scheme would preferably assign a channel to cell x belonging to $F_D(x)$ in order to optimize channel utilization of the cellular system.

When a new call arrives in cell x , the channel allocation algorithm examines the cost of

each available channel $i \in \Lambda(x)$ due to the interfering cell $y \in I(x)$. The allocation cost of the available channel i , $C_x(y, i)$, is defined as

$$C_x(y, i) = v_y(i) + 2[1 - q_y(i)], \quad \forall y \in I(x) \quad (2.7)$$

where $v_y(i)$ and $q_y(i)$ are given by

$$v_y(i) = \begin{cases} 1, & \text{if } i \in \Lambda(y) \\ 0, & \text{otherwise} \end{cases} \quad (2.8)$$

$$q_y(i) = \begin{cases} 0, & \text{if } i \in F_D(y) \\ 1, & \text{otherwise.} \end{cases} \quad (2.9)$$

From (2.7), the allocation cost of the available channel can only yield four different values:

$$C_x(y, i) = \begin{cases} 0, & \text{if } i \notin \Lambda(y) \text{ and } i \notin F_D(y) \\ 1, & \text{if } i \in \Lambda(y) \text{ and } i \notin F_D(y) \\ 2, & \text{if } i \notin \Lambda(y) \text{ and } i \in F_D(y) \\ 3, & \text{if } i \in \Lambda(y) \text{ and } i \in F_D(y). \end{cases} \quad (2.10)$$

The overall cost function of the channel allocation is expressed as

$$C_x(i) = q_x(i) + \sum_{y \in I(x)} \{C_x(y, i)\}, \quad \forall i \in \Lambda(x). \quad (2.11)$$

From (2.11), the term $q_x(i)$ corresponds to the nominal channel condition so that the cost function tends to assign channel i to a new call where channel i belongs to $F_D(x)$. When a call arrives in cell x , the DCA scheme assigns channel i^* , ($i^* \in \Lambda(x)$), such that,

$$C_x(i^*) = \min_{i \in \Lambda(x)} \{C_x(i)\}, \quad (2.12)$$

temporarily to cell x . If there is more than one candidate channel with the minimum cost, one of them is chosen at random.

When a call is terminated in cell x , the DCA scheme performs the channel de-allocation algorithm to release a used channel in order to reduce the mismatching with the optimal FCA channel distribution and to free the channel that becomes available in the greatest number of $I(x)$. In the channel de-allocation algorithm, the cost of each used channel $j \in A(x)$ is examined due to the interfering cell $y \in I(x)$. The de-allocation cost of the used channel j , $R_x(y, j)$, is given by

$$R_x(y, j) = b_x(y, j) + 2q_y(j), \quad \forall y \in I(x) \quad (2.13)$$

where $b_x(y, j)$ is defined as

$$b_x(y, j) = \begin{cases} 0, & \text{if channel } j \text{ is locked in cell } y \\ & \text{only by the allocation in cell } x \\ 1, & \text{otherwise.} \end{cases} \quad (2.14)$$

From (2.13), there are only four values for the de-allocation cost of the used channel:

$$R_x(y, j) = \begin{cases} 0, & \text{if } j \in \Lambda_x(y, j) \text{ and } j \in F_D(y) \\ 1, & \text{if } j \notin \Lambda_x(y, j) \text{ and } j \in F_D(y) \\ 2, & \text{if } j \in \Lambda_x(y, j) \text{ and } j \notin F_D(y) \\ 3, & \text{if } j \notin \Lambda_x(y, j) \text{ and } j \notin F_D(y) \end{cases} \quad (2.15)$$

where $\Lambda_x(y, j)$ represents the set of channels becoming available in cell y when channel j is

released in cell x . Equations (2.10) and (2.15) shows that there is a perfect complementarity between the channel allocation cost contribution $C_x(y, i)$ and the channel de-allocation cost contribution $R_x(y, j)$. When a call is terminated, the channel de-allocation algorithm releases a used channel which becomes available in the greatest number of interfering cells and reduces the mismatching with the optimal FCA channel distribution. The overall cost function of the channel de-allocation is expressed as

$$R_x(j) = 1 - q_x(j) + \sum_{y \in I(x)} \{R_x(y, j)\}, \quad \forall j \in A(x). \quad (2.16)$$

The term $1 - q_x(j)$ shown in (2.16) demonstrates that the cost function prefers to release channel j which does not belong to $F_D(x)$. The de-allocation algorithm releases channel j^* such that

$$R_x(j^*) = \min_{j \in A(x)} \{R_x(j)\}. \quad (2.17)$$

To simplify the implementation of the channel allocation and de-allocation algorithms, $\Lambda(x)$, $\Lambda(y)$, and $A(x)$ are updated when a new call arrives or a call is terminated.

2.2.5 Dynamic Channel Assignment Scheme Using Hopfield Neural Network

In order to increase the capacity of cellular communication systems, a Hopfield neural network [13] can be used in the DCA scheme for optimizing the channel allocation. DCA schemes based on an energy function whose minimization yields the channel allocation are described in [14, 15]. The Hopfield neural network is used to optimize the energy function for

allocating a channel. In [15], hard and soft conditions are formulated in the energy function. The hard condition refers to a violation of co-channel interference constraints. The most important soft conditions for the energy function are the packing condition and the resonance condition. With the packing condition, the allocation solutions tend to use the minimum number of channels to satisfy the global channel demand. With the resonance condition, the scheme tends to assign the same channels to the cells which belong to the same reuse scheme.

Chapter 3 Description of the Proposed DCA Scheme

In a cellular communication system, each mobile call is served by an BS which provides radio access between an MS and an MSC. Within the BS's service coverage area, the MS can establish an acceptable quality communication link that is often comparable to that of landline telephone systems. Because of the rapid growth of the mobile user population, cellular systems must accommodate a large number of mobile users and provide an acceptable signal quality over a large geographic area within a limited frequency spectrum. To achieve an efficient utilization of the radio spectrum, a channel assignment scheme that is consistent with the objectives of increasing capacity and minimizing interference is required.

In Chapter 2, we have reviewed different FCA and DCA schemes and looked at important parameters for channel allocation and de-allocation algorithms. Unlike the channel assignment schemes reviewed in Section 2.2, the proposed DCA scheme does not allocate a group of nominal channels to each cell. Because the initiation of new call arrivals for service from cell to cell is a random process, the distance between two cells using the same channel may be greater than the minimum reuse distance D . With the resonance condition in the cost function, the proposed scheme assigns the same channels to cells so that the distance between the two nearest cells is close to the minimum reuse distance D . Furthermore, a cell is allowed to borrow a channel from the available channel set of its neighboring cells¹ when the cell has no free available channel. The channel assignment is performed in each BS by exchanging status information between BS's. The proposed DCA scheme described in this chapter attempts to increase the traffic-carrying capacity

¹ For simplicity in describing the proposed DCA scheme, the use of the phrase "borrow from cell x " always means to borrow a channel from the available channel set of cell x .

and simplify the channel assignment scheme.

3.1 Proposed Dynamic Channel Assignment Scheme

The proposed DCA scheme consist of three phases: channel allocation, channel de-allocation, and channel borrowing and re-assignment. Cost functions for channel allocation and de-allocation are used to evaluate the cost of using each of the available channels and releasing each of the used channels respectively. With the channel borrowing and re-assigning strategy, a cell is allowed to borrow a channel from its neighboring cells when the available channel set of the cell is empty.

3.1.1 Channel Allocation Algorithm

A cost function is applied in the channel allocation to assign a channel to a new call from the available channel set of cell x . The cost of channel allocation is determined by three decision conditions: co-channel interference condition, interfering-cell available channel condition, and resonance condition:

- The co-channel interference condition ensures that the same channel cannot be used in two interfering cells. The channel allocation algorithm assigns a channel to a new call from the available channel set $\Lambda(x)$ of cell x . If $\Lambda(x)$ is empty, the channel borrowing and re-assigning strategy is performed.

- With the interfering-cell available channel condition, we tend to assign a channel to a cell which minimizes the decrease of the available channel set of its interfering cells. Channel $i \in \Lambda(x)$ is assigned to cell x if the number of the interfering cells $y \in I(x)$ having channel i in $\Lambda(y)$ is minimized.
- With the resonance condition, we tend to assign the same channels to cells which are at the minimum reuse distance, D , apart.

The channel allocation algorithm examines the cost of each available channel i due to its interfering cell $y \in I(x)$ and its co-channel cell $z \in L(x)$. The co-channel cell set $L(x)$ is a set of cells separated by the minimum reuse distance D . The overall cost function of the channel allocation, $C_x(i)$, is given by

$$C_x(i) = \sum_{y \in I(x)} v_y(i) + \sum_{z \in L(x)} w_z(i), \quad \begin{array}{l} \forall i \in \Lambda(x) \\ \forall y \in I(x) \\ \forall z \in L(x) \end{array} \quad (3.1)$$

where $v_y(i)$ and $w_z(i)$ are given by

$$v_y(i) = \begin{cases} 1, & \text{if } i \in \Lambda(y) \\ 0, & \text{otherwise} \end{cases} \quad (3.2)$$

$$w_z(i) = \begin{cases} 0, & \text{if } i \in A(z) \\ 1, & \text{otherwise.} \end{cases} \quad (3.3)$$

From (3.1), the first term, $\sum_{y \in I(x)} v_y(i)$, is used to assign a channel with the interfering-cell

available channel condition while the second term, $\sum_{z \in L(x)} w_z(i)$, represents the resonance condition. When a call arrives in cell x , the DCA scheme assigns channel i^* , ($i^* \in \Lambda(x)$), such that,

$$C_x(i^*) = \min_{i \in \Lambda(x)} \{C_x(i)\}, \quad (3.4)$$

temporarily to cell x . The available channel set $\Lambda(x)$ and the used channel set $A(x)$ are updated after channel i^* is assigned to cell x . Because channel i^* is assigned to cell x , the available channel set of cell y , $\Lambda(y)$, $y \in I(x)$, needs to be updated. Figure 3.1 shows the flowchart of the channel allocation with the channel borrowing and re-assigning strategy. If there is more than one candidate channel with the minimum cost, one of them is chosen at random.

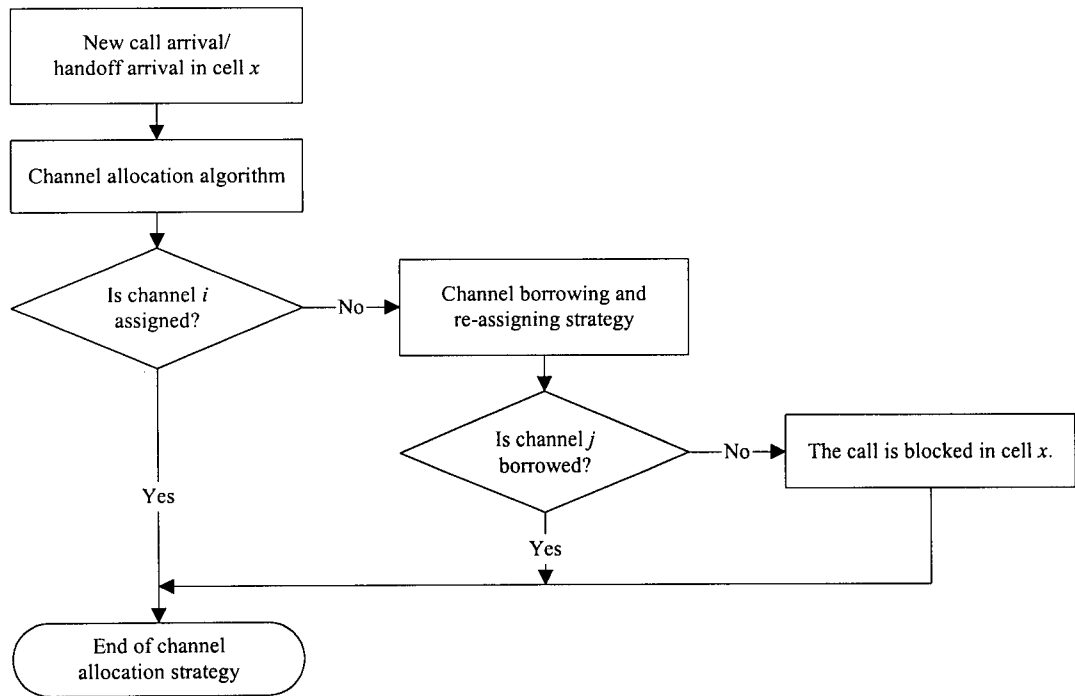


Figure 3.1: Channel Allocation with Channel Borrowing and Re-assigning Strategy.

In Figure 3.1, channel i is assigned to cell x if $\Lambda(x)$ is not empty; otherwise, channel j borrowed from cell $y \in I(x)$ is assigned to cell x by the channel borrowing and re-assigning strategy. Unlike the DCA scheme in [10], the call is only blocked if no such channel can be borrowed. The channel borrowing and re-assigning strategy is an important component in improving the capacity of the cellular communication system because it allows a cell to share a channel from its neighboring cells. The channel borrowing and re-assigning strategy is described in Section 3.1.2.

3.1.2 Channel Borrowing and Re-assigning Strategy

When a call arrives in cell x , a channel chosen from the available channel set $\Lambda(x)$ is assigned to it by using the channel allocation algorithm. In the DCA scheme described in [10], a call in cell x is blocked if cell x has an empty available channel set. Furthermore, the number of channels available in $I(x)$ after the channel allocation in cell x is not considered in the DCA scheme in [10].

The proposed channel borrowing and re-assigning strategy allows cell x to borrow a channel from its neighboring cells $I(x)$ when $\Lambda(x)$ contains no free channel available. With the channel borrowing strategy, a borrowable channel to cell x is generally selected from an adjacent cell which has the largest available channel set, by using the channel allocation algorithm.

Let us consider Figure 3.2 and assume that a new call arrives in cell x and the available channel set of cell x is empty. In Figure 3.2(a), cell x may borrow channel i from cell y (first tier

cell). However, this causes a violation of co-channel interference constraints because channel i is used in cells z_1 and z_2 , $z_1, z_2 \in I(x)$. In order to satisfy the co-channel interference constraints, the channel re-assigning strategy must be performed in cells z_1 and z_2 before cell x is allowed to borrow channel i . With the channel re-assigning strategy in cells z_1 and z_2 , the call served by channel i is switched to another available channel, j , and channel i is released. After channel i is successfully released in cells z_1 and z_2 , cell x can use channel i which is borrowed from cell y . If the channel re-assigning strategy in cells z_1 and z_2 fails, channel i cannot be borrowed from cell y .

As shown in Figure 3.2(b), cell x can also borrow a channel from the available channel set of its neighboring cells in the second tier. In this case, the maximum number of cells which require channel re-assignment is at most three. The flowchart of the channel borrowing and re-assigning strategy is described in Figure 3.3.

In Figure 3.3, the channel re-assigning strategy is performed in cells $D(x) \subset I(x)$ where channel i is used in cells $D(x)$. After channel i is switched to channel $j \in \Lambda(z)$ (cell $z \in D(x)$) and channel i is set free, cell x can borrow channel i from cell y . The new call in cell x is blocked if the channel borrowing and re-assigning strategy is failed. In the proposed DCA scheme, a channel can be used in any cell as long as co-channel interference constraints are satisfied. The capacity of the cellular communication is improved because a cell is allowed to borrow a channel from the available channel set of its neighboring cells by using the channel borrowing and re-assigning strategy.

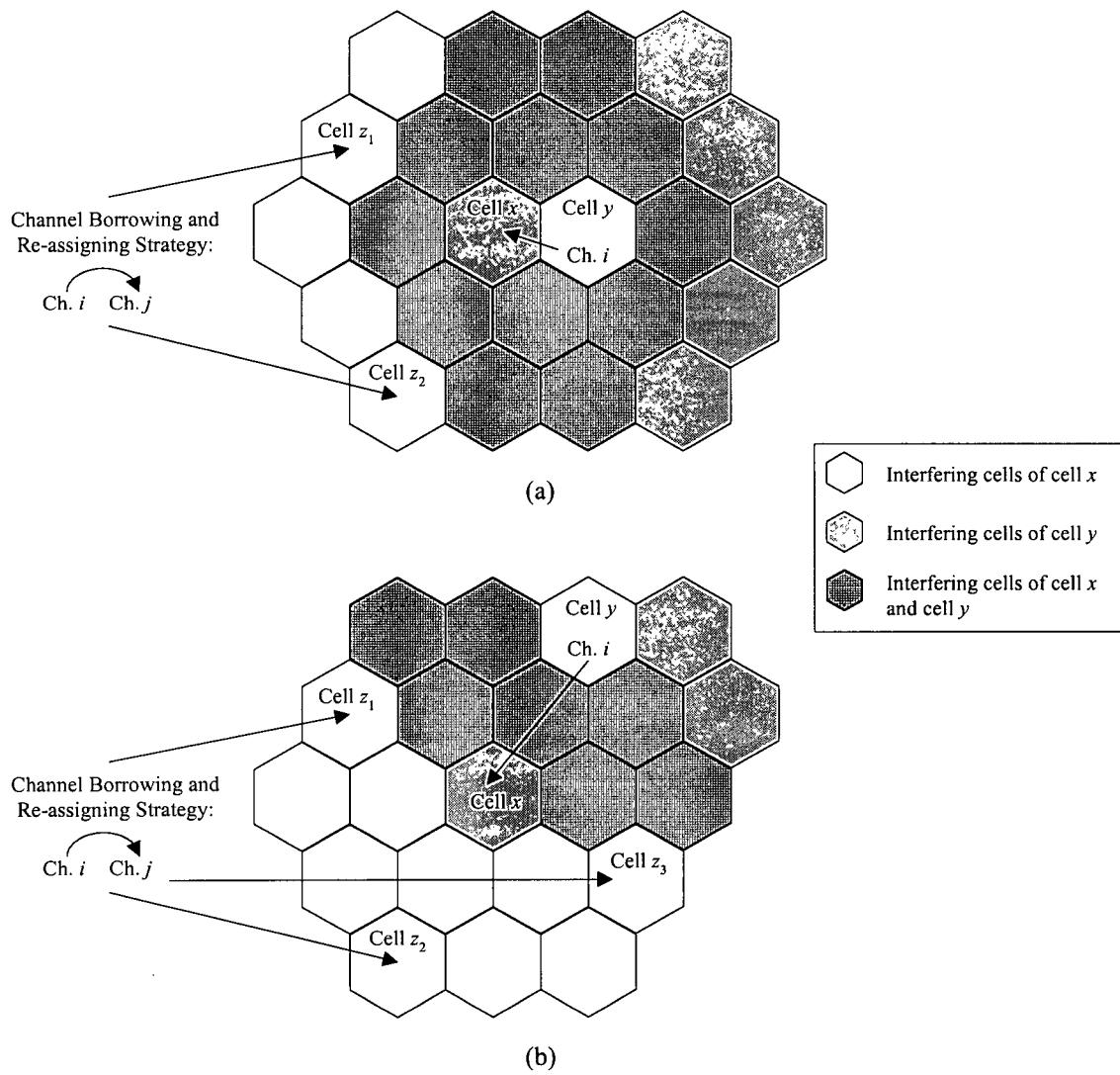


Figure 3.2: Channel Borrowing and Re-assigning Strategy: (a) Borrow from the First Tier Cell, (b) Borrow from the Second Tier Cell.

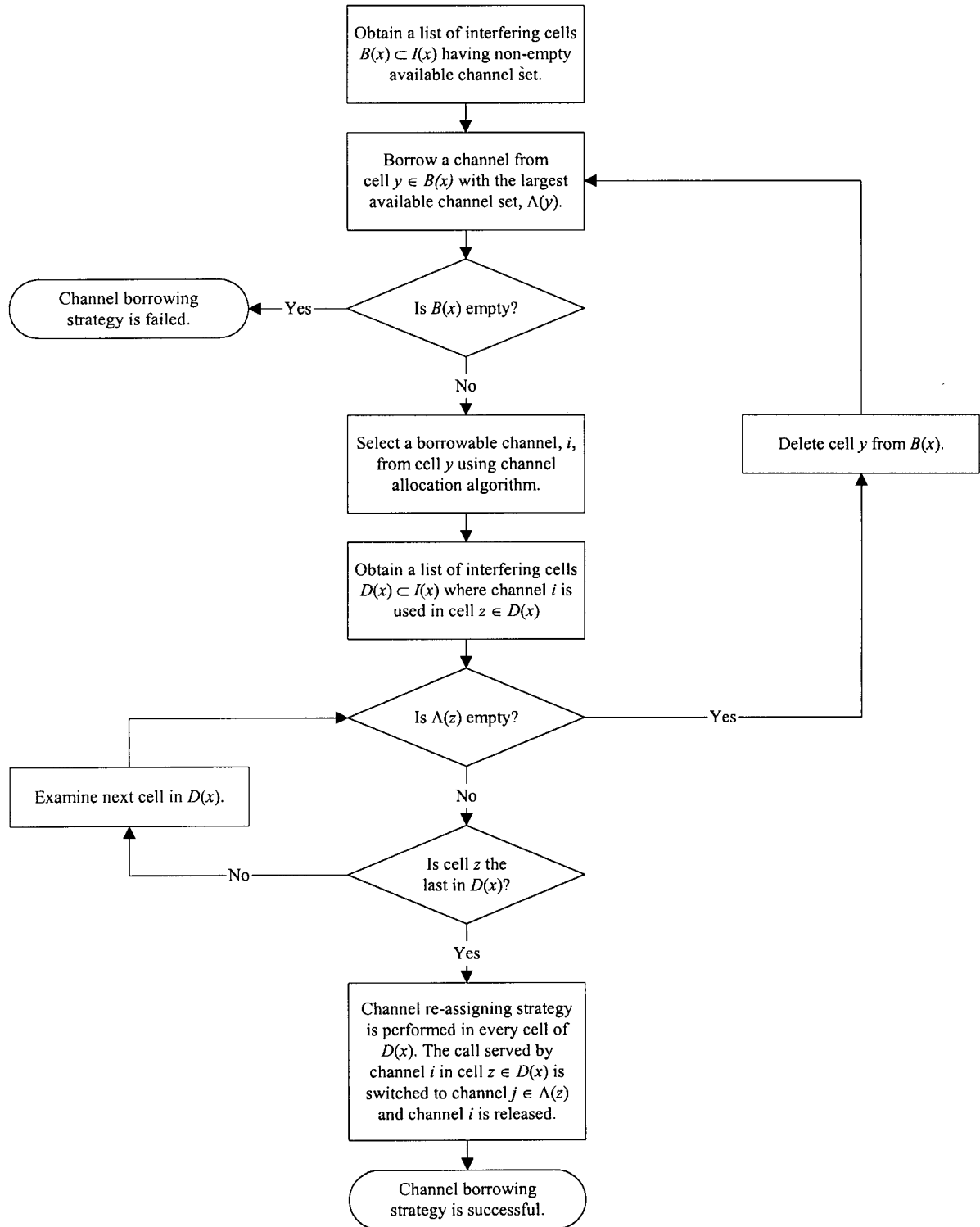


Figure 3.3: Channel Borrowing and Re-assigning Strategy.

3.1.3 Channel De-allocation Algorithm

The objective of the channel de-allocation algorithm is to release a channel from the used channel set $A(x)$ which becomes available in the greatest number of $I(x)$. Similarly, the cost of channel de-allocation is determined by the interfering-cell available channel condition and the resonance condition:

- With the interfering-cell available channel condition, we tend to release a channel to a cell which becomes available in the greatest number of interfering cells.
- With the resonance condition, we tend to release a channel for which the number of co-channel cells using that same channel is minimum.

In the channel de-allocation algorithm, the cost of each used channel $j \in A(x)$ due to its interfering cell $y \in I(x)$ and its co-channel cell $z \in L(x)$ is examined. The overall cost function of the channel allocation, $R_x(j)$, is defined as

$$R_x(j) = \sum_{y \in I(x)} b_x(y, j) + \sum_{z \in L(x)} 1 - w_z(j), \quad \begin{array}{l} \forall j \in A(x) \\ \forall y \in I(x) \\ \forall z \in L(x) \end{array} \quad (3.5)$$

where $b_x(y, j)$ is defined as

$$b_x(y, j) = \begin{cases} 0, & \text{if channel } j \text{ is locked in cell } y \\ & \text{only by the allocation in cell } x \\ 1, & \text{otherwise.} \end{cases} \quad (3.6)$$

The first term $\sum_{k \in I(x)} b_x(y, j)$ shown in (3.5) examines the availability of channel j in the interfer-

ing cell $y \in I(x)$ when channel j is released in cell x . The second term, $\sum_{z \in L(x)} 1 - w_z(j)$, is used to release a channel with the resonance condition. When a call is terminated, the channel de-allocation algorithm releases a channel which becomes available in the greatest number of its interfering cells. The channel de-allocation algorithm releases channel j^* such that

$$R_x(j^*) = \min_{j \in A(x)} \{R_x(j)\}. \quad (3.7)$$

After channel j^* is set free in cell x , $\Lambda(x)$, $A(x)$, and $\Lambda(y)$ are updated. The channel de-allocation algorithm of the proposed DCA scheme is presented in Figure 3.4. A call departure occurs when a mobile user is handed off from one cell to its neighboring cell.

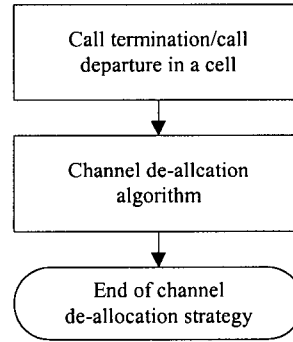


Figure 3.4: Channel De-allocation Algorithm.

To simplify the implementation of channel allocation and de-allocation algorithms, $\Lambda(x)$, $\Lambda(y)$, and $A(x)$ are updated only when a new call arrives or a call is terminated.

3.2 Summary

In this chapter, the proposed DCA scheme with channel borrowing and re-assignment was presented. The proposed scheme consists of channel allocation, channel de-allocation, and channel borrowing and re-assignment. Because the channel borrowing and re-assigning strategy allows a cell to borrow a channel from its neighboring cells, it can improve the capacity of the cellular system and adapt to changing traffic conditions as well as user distributions. The next chapter compares the performance of the proposed DCA scheme to some previously studied channel assignment schemes.

Chapter 4 Performance Results with No Handoff

In this chapter, computer simulation results of the performance of the proposed DCA scheme are presented. The results are in terms of blocking probabilities with uniform and non-uniform traffic distributions. We also investigate the effects of operational parameters used in the cost functions of the channel allocation and de-allocation algorithms in order to simplify the proposed scheme. The results are also compared with those of some previously studied channel assignment schemes.

4.1 Simulation Model

The simulation model consists of a parallelogram-shaped network of hexagonal cells, call arrival and call duration models, and channel allocation and de-allocation algorithms. Mobile calls arrive at random to a cell in the cellular network according to a Poisson process. When a call arrives at a cell, the channel allocation algorithm of the proposed DCA scheme is applied to assign a channel to the call. In the simulation model, call durations are assumed to be independent and exponentially distributed. The channel de-allocation algorithm is performed whenever the call is terminated in the cell or the call is handed off to another cell.

4.1.1 Cellular System Layout

In order to investigate the performance of the proposed DCA scheme, a cellular system which contains 49 hexagonal cells is used for the computer simulation. Figure 4.1 shows the

parallelogram-shaped cellular network of hexagonal cells [7, 8, 10, 15]. Each side of the parallelogram-shaped network contains 7 cells while the edge of each hexagonal cell is of length R . In our simulation, parameters i and j are chosen to be 2 and 1 respectively so that from (2.4), the frequency reuse factor N is 7. The distance between two nearest co-channel BS's obtained from (2.3) is $D = \sqrt{21}R$. Once channel i is allocated to cell x , it cannot be reused in two tiers of cells adjacent to cell x because of unacceptable co-channel interference levels.

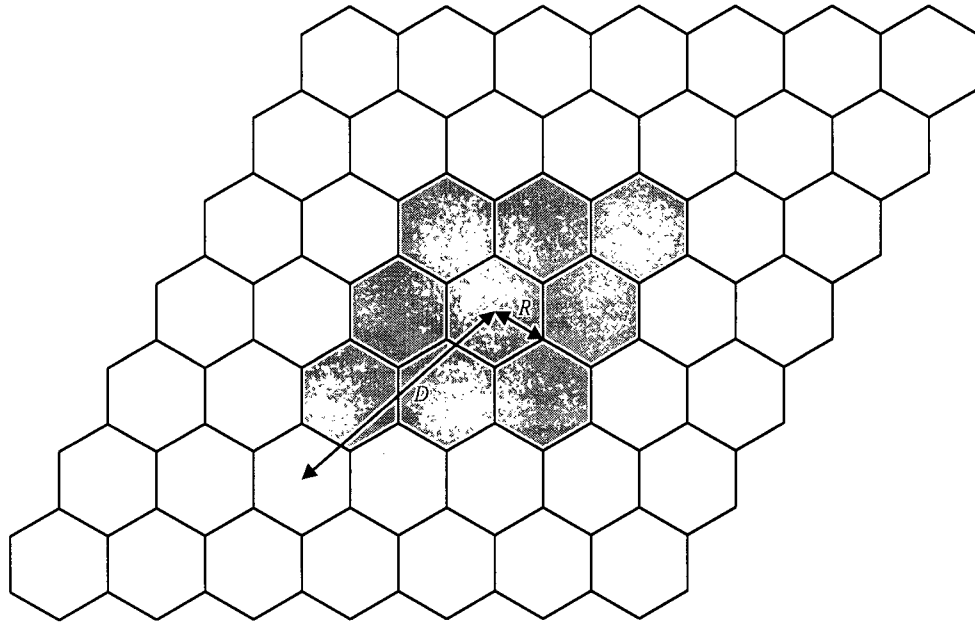


Figure 4.1: Cellular System for Simulation of the Proposed DCA Scheme.

In the 49 hexagonal cell network, only the central 9 cells have a complete set of interfering cells (i.e., the total number of interfering cells = 18) which consists of two tiers of neighboring cells (i.e., $N = 7$). Cells which have an incomplete set of interfering cells generally have a lower blocking probability than the central 9 cells. For the simulation, the total number, M , of available channels is 70.

4.1.2 Call Arrival and Call Duration Models

The arrival of calls follows a Poisson process and the call duration is exponentially distributed with a mean of T_m . To examine the performance of the proposed DCA scheme, computer simulations of call arrival and call duration models are used with the following parameters:

- New call arrivals in any hexagonal cell form a Poisson process with a mean call arrival rate λ_n while handoff calls arrive with a mean handoff call arrival rate λ_h .
- The call duration τ is exponentially distributed with an expected value of $T_m = \frac{1}{\mu}$ and the mean outgoing handoff rate per calling mobile is μ_h .

The mean call arrival rate in a cell is the sum of the new call arrival rate and handoff call arrival rate

$$\lambda_t = \lambda_n + \lambda_h \quad (4.1)$$

while the mean call departure rate is the sum of the rates due to terminations from call completions and handoffs

$$\mu_t = \mu + \mu_h. \quad (4.2)$$

The new arrival traffic intensity per cell and total traffic intensity per cell are defined as $\lambda_n T_m$ and

$\frac{\lambda_t}{\mu_t}$ respectively. In our simulation, the mean call duration time, T_m , is assumed to be 2 minutes.

4.1.3 Performance Measures for Channel Assignment Schemes

The performance of the proposed DCA scheme will be evaluated through the new call blocking probability, the handoff blocking probability, the dropped call probability, and the total call blocking probability. These four blocking probabilities are obtained using the following formulas:

(1) New call blocking probability (P_{bn})

$$P_{bn} = \frac{\text{number of new calls blocked in the cell}}{\text{total number of calls generated in the cell}} \quad (4.3)$$

(2) Handoff blocking probability (P_{bh})

$$P_{bh} = \frac{\text{number of handoff failures in the cell}}{\text{total number of handoff attempts in the cell}} \quad (4.4)$$

(3) Dropped call probability (P_{dc})

$$P_{dc} = \frac{\text{number of handoff failures in the cell}}{\text{total number of calls generated in the cell}} \quad (4.5)$$

(4) Total call blocking probability (P_b)

$$\begin{aligned} P_b &= \frac{\text{number of new calls blocked} + \text{number of handoff failures in the cell}}{\text{total number of calls generated in the cell}} \\ &= P_{bn} + P_{dc} \end{aligned} \quad (4.6)$$

In this chapter, the performance of the proposed DCA scheme is evaluated assuming that a mobile stays in the same cell throughout the duration of a call. In this case, the cellular system has no handoffs or handoff failures, and thus P_{bn} is the same as P_b . The simulation results of the proposed scheme with possible handoffs are presented in Chapter 5. The simulation results

presented in this chapter have 99% confidence intervals of at most $\pm 7\%$ of the values shown. For traffic intensity values greater than 8, the 99% confidence intervals are at most $\pm 5\%$.

4.2 Operational Parameters for Channel Allocation and De-allocation

To develop the simplified DCA scheme, we examine the operational parameters for the channel allocation and de-allocation algorithms. In this section, the effects of nominal channel condition and the resonance condition on the proposed DCA scheme are investigated.

4.2.1 Nominal Channel Condition

In [10], the nominal channel condition is applied in the channel allocation and de-allocation algorithms. The DCA scheme in [10] initially allocates a set of nominal channels $F_D(x)$ to each cell x . With the nominal channel condition, we tend to assign channel i to cell x where channel i belongs in $F_D(x)$. To examine the effect of the nominal channel condition, the channel allocation and de-allocation cost functions shown in (3.1) and (3.5) are modified by adding a term for the nominal channel condition. The modified channel allocation and de-allocation cost functions are as follows

$$C'_x(i) = C_x(i) + \underbrace{\left\{ q_x(i) + \sum_{y \in I(x)} \alpha [1 - q_y(i)] \right\}}_{\text{Nominal Channel Condition}}, \quad \begin{array}{l} \forall i \in \Lambda(x) \\ \forall y \in I(x) \end{array} \quad (4.7)$$

$$R'_x(j) = R_x(j) + \underbrace{\left\{ 1 - q_x(j) + \sum_{y \in I(x)} \alpha q_y(j) \right\}}_{\text{Nominal Channel Condition}}, \quad \begin{array}{l} \forall j \in A(x) \\ \forall y \in I(x) \end{array} \quad (4.8)$$

where $q_x(i)$ and $q_y(i)$ are defined in (2.8). The constant coefficient α is the weight of the nominal channel condition in the channel allocation and de-allocation cost functions. The channel allocation algorithm uses (2.11) to assign a channel to a cell while (2.16) is applied in the channel de-allocation algorithm for releasing a channel. To study the effects of nominal channel condition, three values of α are examined in terms of new call blocking probability. The new call blocking probabilities of the central 9 cells as well as all 49 cells with three values of α are shown in Figures 4.2 and 4.3 respectively.

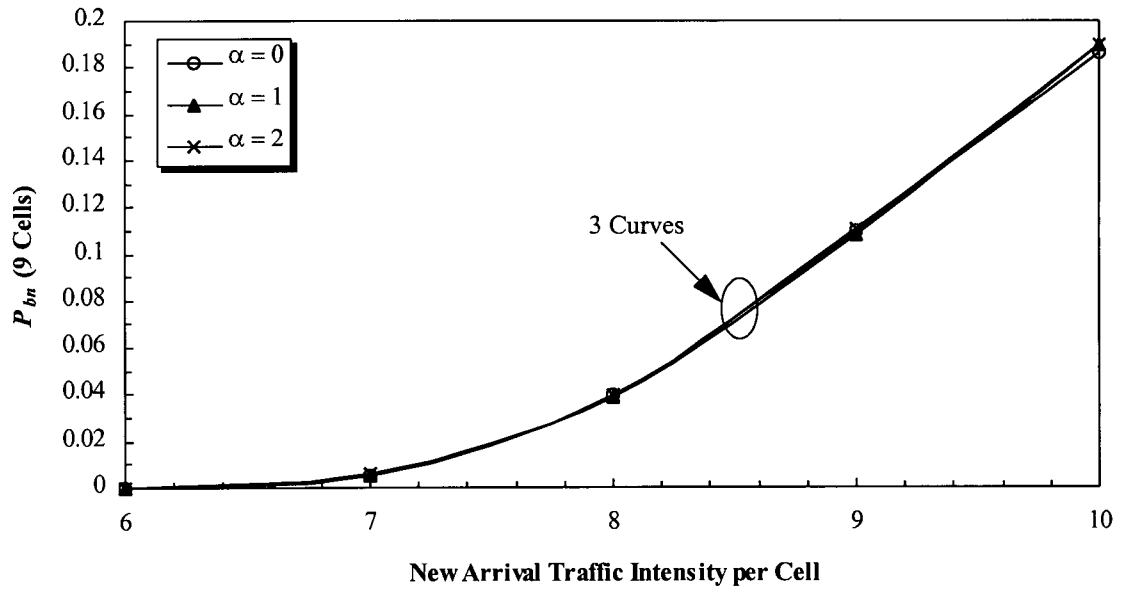


Figure 4.2: Simulation Results of New Call Blocking Probability, P_{bn} , (averaged over central 9 cells) for the Proposed DCA Scheme with (i) $\alpha = 0$, (ii) $\alpha = 1$, and (iii) $\alpha = 2$.

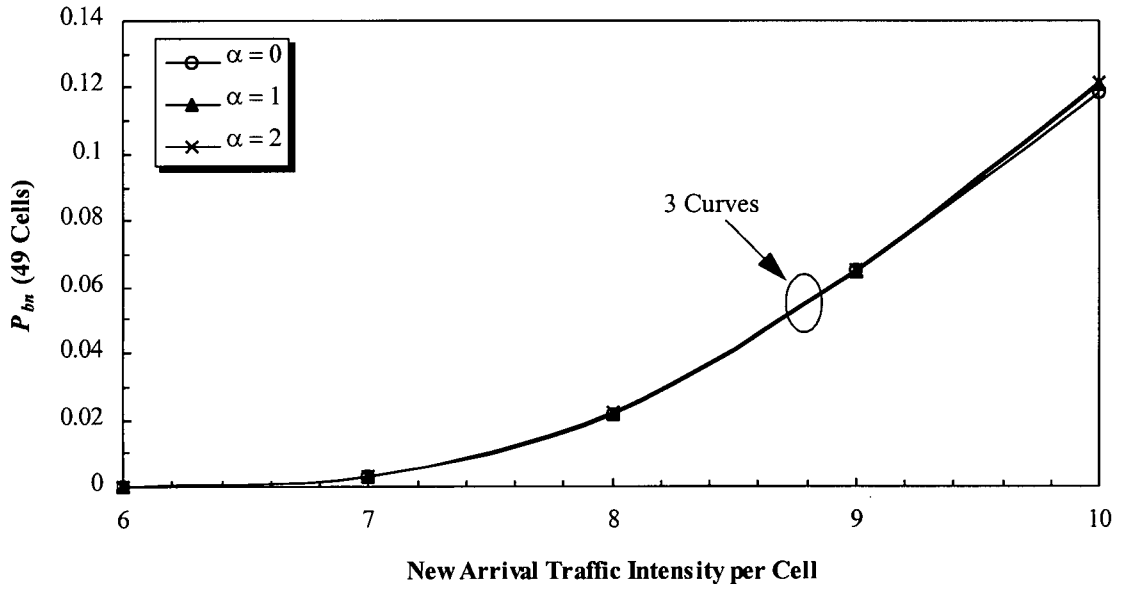


Figure 4.3: Simulation Results of New Call Blocking Probability, P_{bn} , (averaged over 49 cells) for the Proposed DCA Scheme with (i) $\alpha = 0$, (ii) $\alpha = 1$, and (iii) $\alpha = 2$.

Figures 4.2 and 4.3 show that the nominal channel condition (i.e., the weight factor $\alpha > 0$) does not improve P_{bn} of the central 9 cells or of all 49 cells. The simulation results illustrate the interfering-cell available channel condition is one of the important factors for the channel allocation and de-allocation algorithms. In order to simplify the proposed DCA scheme, it is suggested that the nominal channel condition can be omitted from the cost functions of the channel allocation and de-allocation algorithms.

4.2.2 Resonance Condition

As mentioned in Section 2.2.4, the channel allocation and de-allocation cost functions of the DCA [10] scheme only consists of the interfering-cell available channel condition and the

nominal channel condition. The simulation results presented in the previous section demonstrate that the interfering-cell available channel condition is one of the important factors for channel allocation and de-allocation algorithms. In this section, the effect of the resonance condition on the proposed DCA scheme is examined in order to improve the call blocking probability and increase the traffic capacity. With the resonance condition, we tend to assign the same channels to cells which are at the minimum reuse distance, D , apart. The modified channel allocation and de-allocation cost functions, which are used to validate the performance of the proposed scheme with the resonance condition, are given by

$$C_x''(i) = \sum_{y \in I(x)} v_y(i) + \sum_{z \in L(x)} \beta w_z(i), \quad \begin{array}{l} \forall i \in \Lambda(x) \\ \forall y \in I(x) \\ \forall z \in L(x) \end{array} \quad (4.9)$$

$$R_x''(j) = \sum_{y \in I(x)} b_x(y, j) + \sum_{z \in L(x)} \beta [1 - w_z(j)], \quad \begin{array}{l} \forall j \in A(x) \\ \forall y \in I(x) \\ \forall z \in L(x) \end{array} \quad (4.10)$$

where β is a coefficient term for the resonance condition in the channel allocation and de-allocation cost functions. To study the effect of the resonance condition, computer simulations of the proposed DCA scheme with different values of β were run. Figures 4.4 and 4.5 show the new call blocking probability of the central 9 cells and all 49 cells with different values of β .

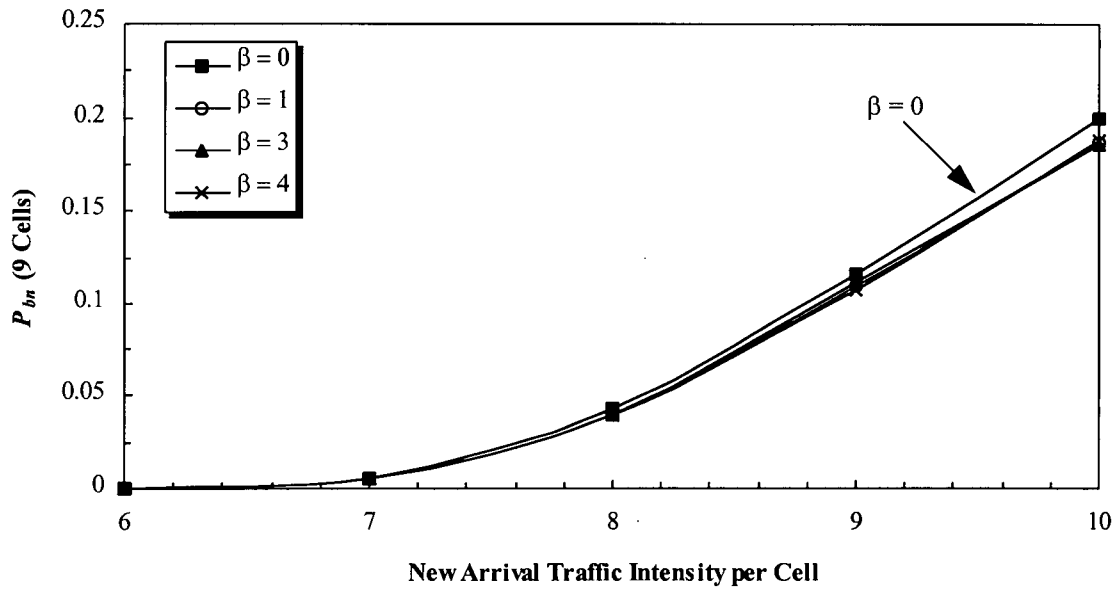


Figure 4.4: Simulation Results of New Call Blocking Probability, P_{bn} , (averaged over central 9 cells) for the Proposed DCA Scheme with (i) $\beta = 0$, (ii) $\beta = 1$, (iii) $\beta = 3$, and (iv) $\beta = 4$.

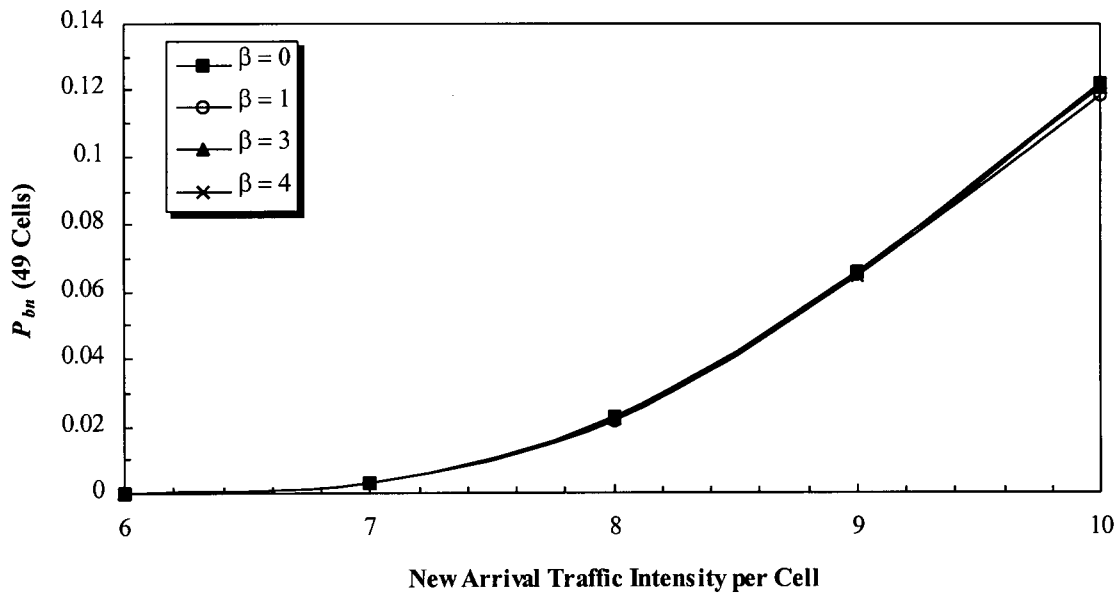


Figure 4.5: Simulation Results of New Call Blocking Probability, P_{bn} , (averaged over 49 cells) for the Proposed DCA Scheme with (i) $\beta = 0$, (ii) $\beta = 1$, (iii) $\beta = 3$, and (iv) $\beta = 4$.

In Figure 4.4, cost functions $C_x''(i)$ and $R_x''(j)$ with $\beta > 0$ has a lower new call blocking probability of the central 9 cells than the functions with $\beta = 0$. As seen in Figure 4.5, the increase in the coefficient β does not improve the new call blocking probability in all of the 49 cells. Figures 4.4 and 4.5 show that the blocking probabilities of the central 9 cells and all 49 cells are not improved where the coefficient β is increased from 1 to 4. For the sake of simplicity, we choose the coefficient β to be 1 for channel allocation and de-allocation cost functions. In summary, the interfering-cell available channel condition and the resonance condition are two important operational parameters for the proposed DCA scheme.

4.3 Results and Discussions

Simulation results of the proposed DCA scheme are presented in terms of call blocking probabilities. The proposed scheme is then compared to some previously studied channel assignment schemes. The results shown in the previous section indicate that two important operational parameters for channel allocation and de-allocation algorithms are the interfering-cell available channel condition and the resonance condition. To compare the proposed scheme with other channel assignment schemes, the simulated cellular system with 49 hexagonal cells (as shown in Figure 4.1) is used. As described in Section 4.1.2, the same call arrival and call departure models are used in the computer simulation of all channel assignment schemes. The arrival of calls is a Poisson process and the call duration is exponentially distributed with a mean of 2 minutes. The comparison between the proposed scheme and other channel assignment schemes are performed for both uniform and non-uniform traffic distributions. In Chapter 5, simulation results of the proposed scheme with handoffs as well as comparison with other schemes are presented.

4.3.1 Uniform Traffic Distribution

In this section, simulation results of the proposed DCA scheme and comparison with other channel assignment schemes for a uniform traffic distribution are shown. In the uniform traffic distribution, all cells have the same new call arrival rate. To examine the performance of the proposed scheme, the simulation results of the proposed scheme are first compared with the FCA [1], the BDCL [7], the CP-DCA [8], the DCA [10] schemes in terms of blocking probabilities for the central 9 cells and all 49 cells in the uniform traffic distribution. As shown in [7], the SB scheme and the BCO scheme always give a higher blocking probability than the BDCL scheme. Therefore, their performances are not shown in our comparison. Figures 4.6 and 4.7 show the simulation results of the new call blocking probability for the central 9 cells and all 49 cells obtained by different channel assignment schemes.

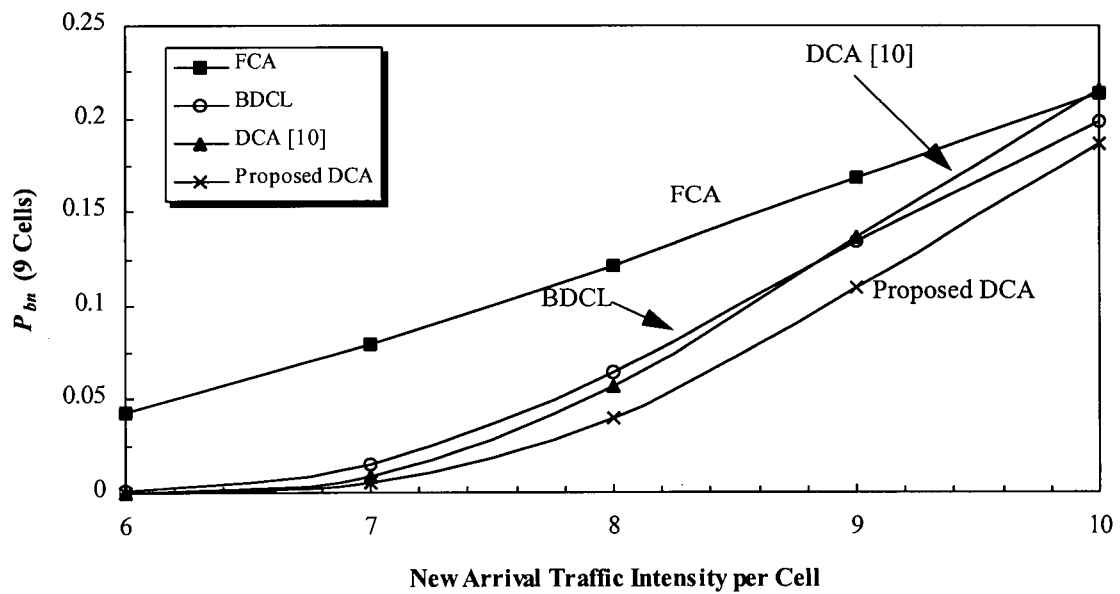


Figure 4.6: New Call Blocking Probability, P_{bn} , (averaged over central 9 cells) with Uniform Traffic Distribution.

The simulation results of FCA scheme agree with the Erlang B formula while the results

of the BDCL and the DCA [10] schemes agree with the values in [7, 8, 10]. From Figure 4.6, in a uniform traffic distribution, the proposed DCA scheme gives the lowest blocking probability for the central 9 cells, followed by the BDCL, the DCA [10], and the FCA schemes. At a traffic intensity of 10, the blocking probabilities of the central 9 cells are 18.5%, 21.5%, 20%, and 21.5% for the proposed DCA scheme, DCA [10], the BDCL, and the FCA schemes respectively. By adding the resonance condition as well as the channel borrowing and re-assigning strategy, the proposed scheme performs better than the DCA scheme shown in [10]. As seen in Figure 4.6, the DCA [10] scheme does not perform better than the BDCL scheme under the uniform traffic distribution when the traffic intensity per cell is greater than 9. The resonance condition and the channel borrowing and re-assigning strategy in the proposed scheme improve the blocking probability of the central 9 cells which have a complete set of interfering cells. The proposed scheme can give a lower blocking probability than the FCA, the BDCL, and the DCA [10] schemes when the cellular system contains more than 49 hexagonal cells. As a result, the channel borrowing and re-assigning strategy reduces the call blocking probability because it allows a cell to borrow a channel from the available channel set of its neighboring cells.

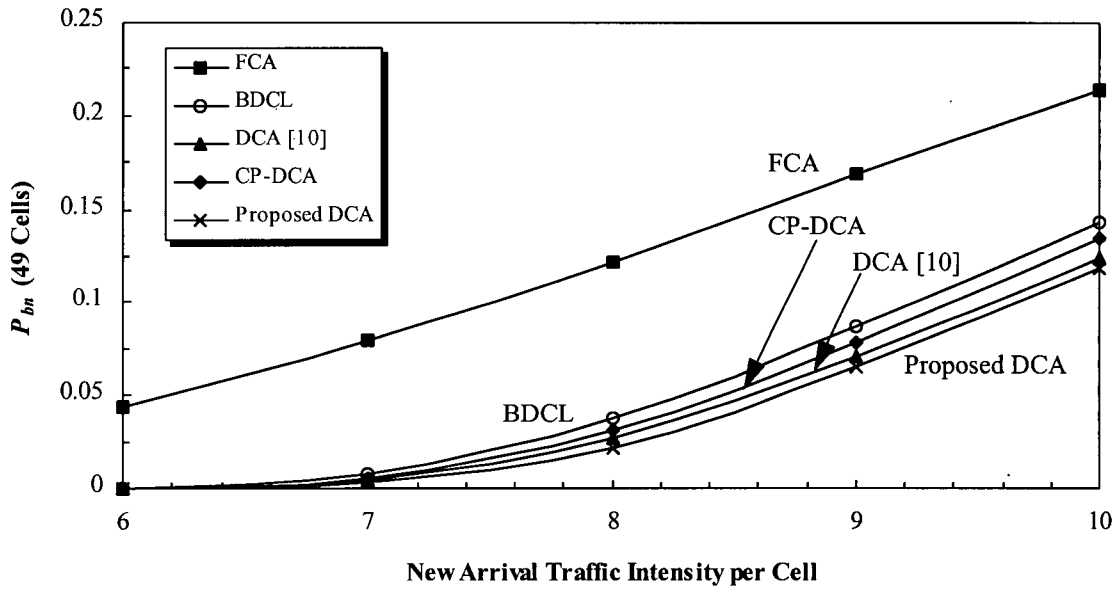


Figure 4.7: New Call Blocking Probability, P_{bn} , (averaged over 49 cells) with Uniform Traffic Distribution.

Figure 4.7 shows the simulation results of P_{bn} with a uniform traffic distribution for the FCA, the BDCL, the CP-DCA, the DCA [10], and the proposed DCA schemes where the P_{bn} is averaged over all 49 cells. The simulation results demonstrate that the proposed DCA scheme has the lowest blocking probability¹. Under heavy traffic conditions (i.e., the traffic intensity is 10), the new call blocking probabilities are 11.7%, 12.5%, 13.5%, 14.4%, and 21.5% for the proposed DCA scheme, the DCA [10], the CP-DCA, the BDCL, and the FCA schemes respectively.

¹ After most of this research work was completed, we found a paper [16] describing a channel assignment scheme based on the BDCL scheme which has similar performance to our proposed scheme.

4.3.2 Call Blocking Distribution

For the simulation, a 49 hexagonal cell cellular network is used so that only the central 9 cells have a complete set of interfering cells (i.e., 18 interfering cells). Because the number of interfering cells for each cell may not be the same, each cell may have a different call blocking probability in a uniform traffic distribution. Cells which have an incomplete set of interfering cells generally have a lower blocking probability than the central 9 cells. In order to study the call blocking distribution, we measure the average blocking probabilities of different tier cells with a uniform traffic distribution. Figure 4.8 shows a parallelogram shaped cellular network contains three tiers of cells. The simulation results of call blocking probability for three tiers are presented in Figure 4.9.

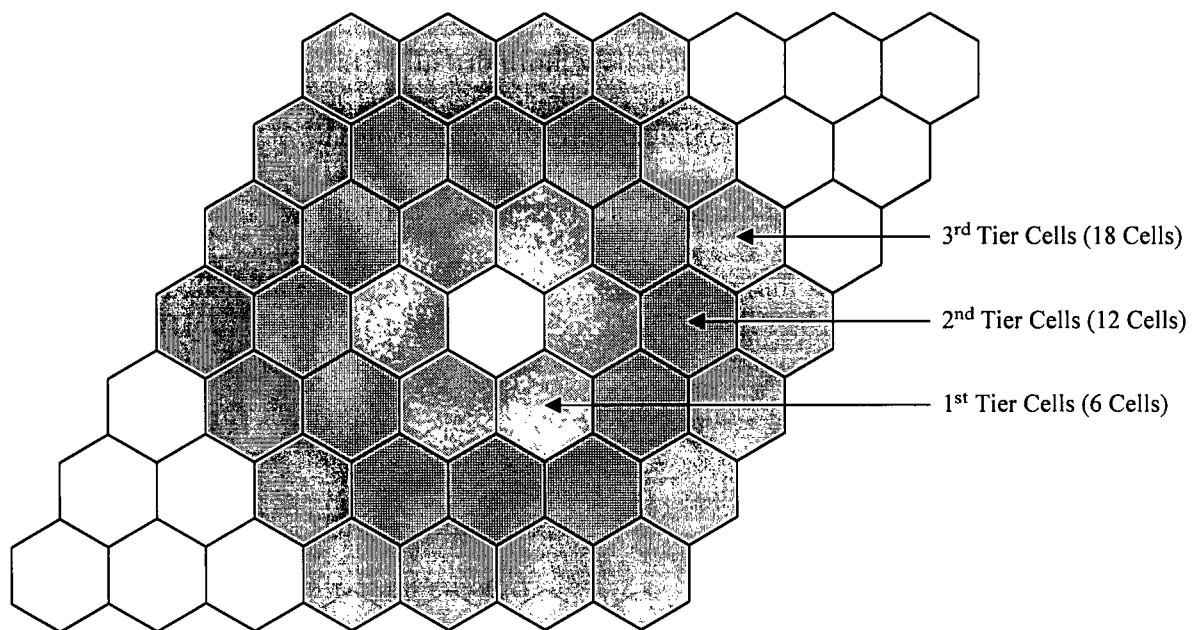


Figure 4.8: Parallelogram-shaped Cellular Network with Three Tiers.

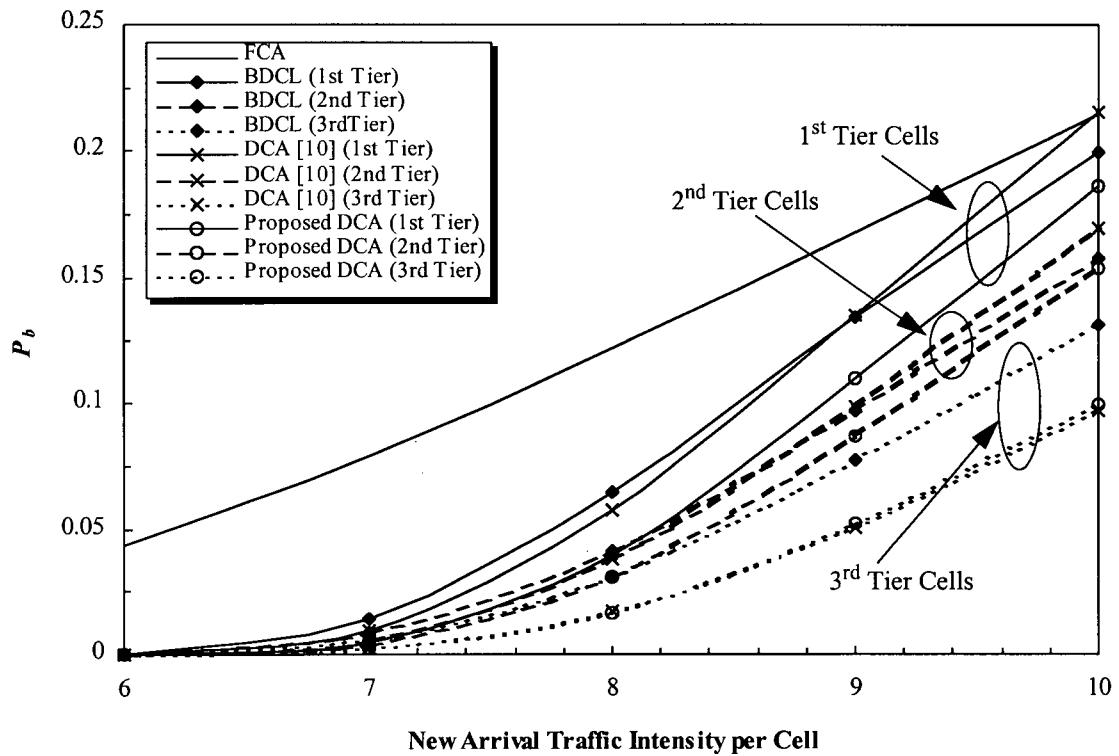


Figure 4.9: Total Call Blocking Probability, P_b , for Three Different Tier Cells with Uniform Traffic Distribution.

As shown in Figure 4.9, the proposed DCA scheme significantly improves the blocking probability for the first tier cells. It also has the lowest average blocking probability in the second tier cells. On the other hand, it performs similarly to the DCA [10] scheme in the third tier cells. Therefore, the addition of the resonance condition and the channel borrowing and re-assigning strategy in the proposed scheme can reduce the blocking probabilities for the first and second tier cells in the 49 cell network.

4.3.3 Non-uniform Traffic Distribution

In practice, the traffic distribution of the cellular system may be non-uniform and depends on the distribution of mobile users. The cellular system being simulated consists of 49 hexagonal cells as shown in Figure 4.1. Traffic distribution patterns A [7] and B [8] are used to study the performance of the proposed DCA scheme with non-uniform traffic distributions. Figure 4.10 shows two cases of non-uniform traffic load where the numbers in the cells represent the Poisson arrival rates (calls/hour) in the respective cells. The call arrival rates range from 20 to 200 calls/hour.

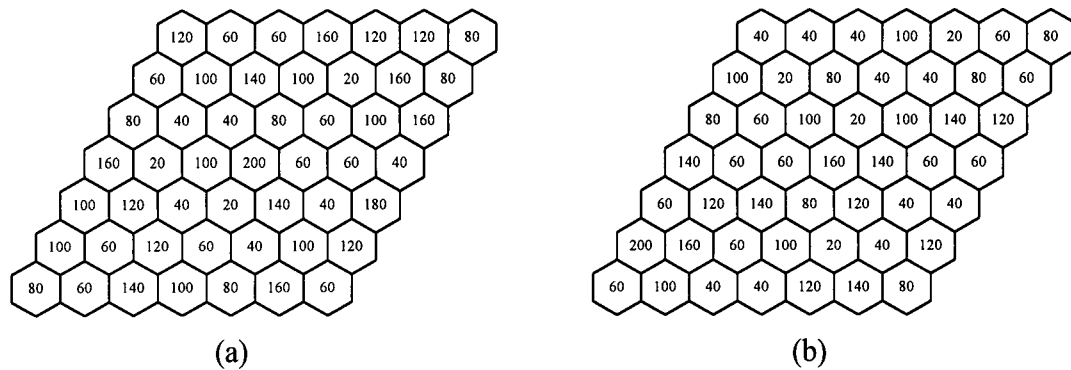


Figure 4.10: Non-uniform Traffic Distribution (calls/hour) in a 49-Cell System: (a) Traffic Distribution Pattern A, (b) Traffic Distribution Pattern B.

The proposed DCA scheme and other channel assignment schemes are simulated by changing the traffic load of the cellular system. The traffic rate for each cell is increased by 0 to 100 percent over the base load which corresponds to an average call arrival rate per cell of 150 calls/hour (i.e., the new arrival traffic intensity per cell is 5). The simulation results are summarized in Figure 4.11 for Pattern A and in Figure 4.12 for Pattern B.

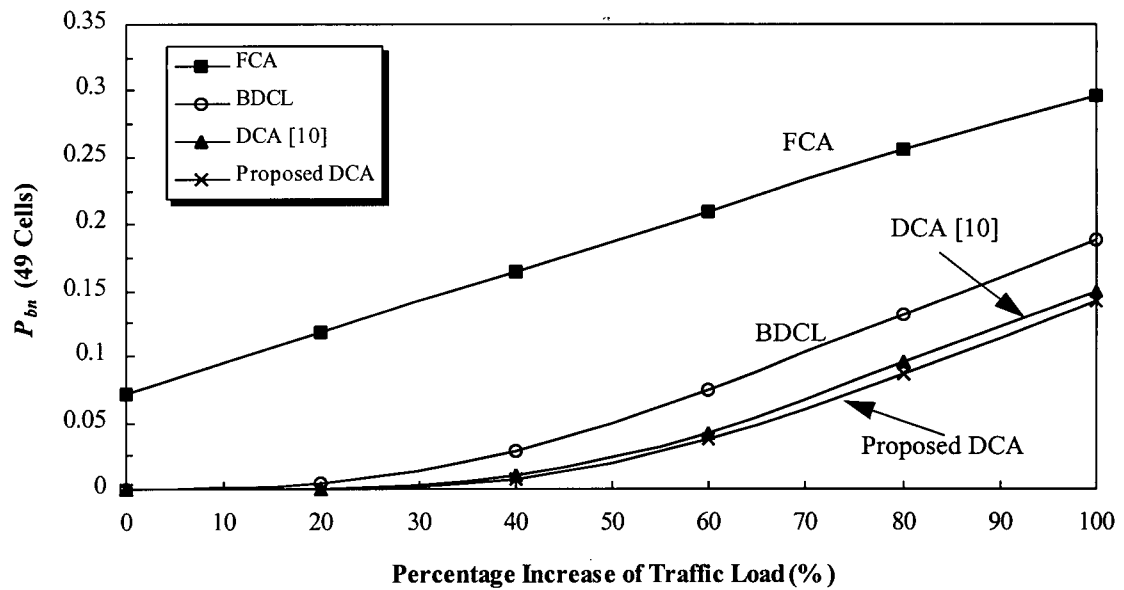


Figure 4.11: New Call Blocking Probability, P_{bn} , (averaged over 49 cells) with Non-uniform Traffic Distribution Pattern A.

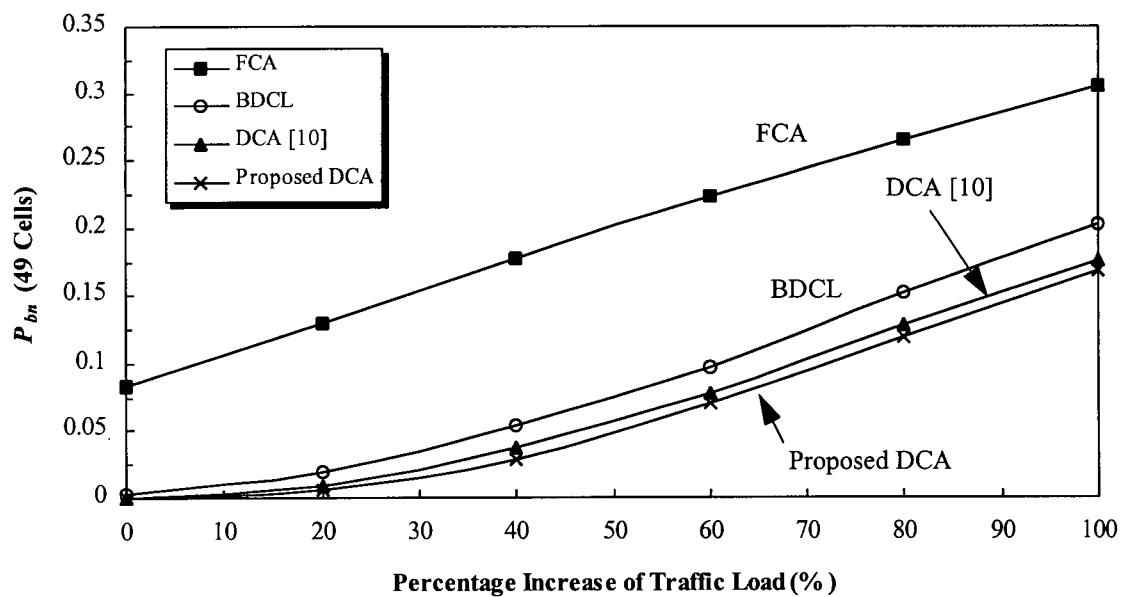


Figure 4.12: New Call Blocking Probability, P_{bn} , (averaged over 49 cells) with Non-uniform Traffic Distribution Pattern B.

In Figures 4.11 and 4.12, the results for the FCA scheme is obtained from the Erlang B formula while the simulation results for the BDCL scheme agree with values in [7, 8]. The results show that the proposed DCA scheme gives the lowest blocking probability, followed by the DCA [10], the BDCL and the FCA schemes. In Figure 4.11, at the base load, the FCA scheme has a blocking probability of 7% while the other three schemes have negligible blocking. Under heavy traffic conditions (100% above the base load), the blocking probabilities are 14.0%, 15.0%, 18.8%, and 29.6% for the proposed DCA, the DCA [10], the BDCL, and the FCA schemes respectively. With the traffic distribution pattern B, Figure 4.12 shows that the blocking probability of the proposed scheme is again lower than those of the other three channel assignment schemes. Hence, the proposed DCA scheme has a better performance than the other three channel assignment schemes for both uniform and non-uniform traffic distributions.

4.4 Summary

Simulation results for the proposed DCA scheme were presented and compared with results for other channel assignment schemes. The effects of operational parameters used in the channel allocation and de-allocation cost functions were also examined. It was found that the two important parameters used in cost functions are the interfering-cell available channel condition and the resonance condition. For both uniform and non-uniform traffic distributions, the proposed DCA scheme has the lowest average blocking probability in the central 9 cells and all 49 cells. Furthermore, the addition of the resonance condition as well as the channel borrowing and re-assigning strategy in the proposed scheme can significantly reduce the blocking probability of the central 9 cells which have a complete set of interfering cells.

Chapter 5 Performance Results with Handoff

When an MS crosses a cell boundary while a call is in progress, a handoff is needed to transfer the call to a new channel available to the new BS. The handoff operation may be caused by radio link degradation and is performed when the link quality between the MS and the BS falls below an acceptable threshold level. The handoff results in overhead associated with assigning and re-assigning communication channels. As cell sizes are reduced for future microcellular systems, mobiles will cross cell boundaries more frequently and the handoff rate will increase so that handoff management will become a more important task. In order to provide high quality and reliable wireless services, handoffs must be successfully performed and be imperceptible to mobile users.

In Chapter 4, the performance of the proposed DCA scheme was compared to some previously studied channel assignment schemes assuming that the MS stays in the same cell throughout the duration of a call. To take into account the effect of call handoffs, two mobility models are used in this thesis to study the performances of the proposed scheme and other channel assignment schemes. In this chapter, we first describe these two mobility models and present approximate and simulation results for blocking probabilities obtained with the FCA scheme and these two mobility models. We then examine the performance of the proposed scheme through computer simulations and compare it to some previously studied channel assignment schemes with these mobility models in both uniform and non-uniform traffic distributions. We also study the effect of the MS maximum speed on the call blocking distributions in the 49 hexagonal cell network.

5.1 Mobility Models

Mobility models, which are used to determine the handoff blocking probability for mobile users, are very important in the performance analysis of cellular networks. Thomas et al. assume that an MS moves in a straight line with a random speed and an independent direction [17]. In the mobility model described in [18], the MS changes its speed and direction randomly when it crosses a cell boundary.

In these mobility models, an BS has signal coverage in a cell of radius R and mobiles are uniformly distributed in the cellular system with a uniform traffic distribution. As described in Section 4.1.2, the call arrival process is Poisson with the same mean arrival rate in all the hexagonal cells while the call duration is random and exponentially distributed. In this thesis, the following two mobility models are used for the performance analysis of the cellular network. Figure 5.1 show mobile motion examples in Mobility Model A and B.

(1) Mobility Model A [17]

The speed and direction of an MS are independent random variables. The MS moves in a straight line without changing its speed and direction. The speed and direction are uniformly distributed in $(0, V_{\max})$ and $(0, 2\pi)$ respectively where V_{\max} is the maximum speed of the MS. See Figure 5.1(a).

(2) Mobility Model B [18]

The speed and direction of an MS are independent random variables. The speed and direction are regenerated randomly and independently when the MS crosses a cell boundary. The new direction is uniformly distributed in $\left(-\frac{\pi}{2}, \frac{\pi}{2}\right)$ relative to the normal direction of the boundary

entering the new region. See Figure 5.1(b).

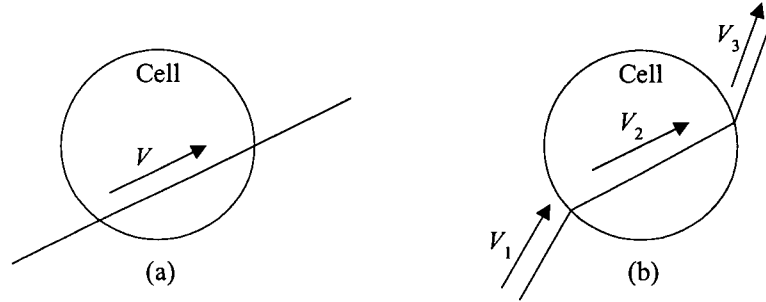


Figure 5.1: Mobile Motion Examples: (a) Mobility Model A, (b) Mobility Model B.

In Mobility Model A described in [17], the mean boundary crossing rate per mobile, μ_b , in an arbitrary cell in terms of mean vehicle speed $E[V]$ is given by

$$\mu_b = \frac{E[V]L}{\pi A} \quad (5.1)$$

where A and L are the area and the perimeter length of the circular-shaped cell respectively. The parameters A and L are given by

$$A = \pi R^2 \quad (5.2)$$

$$L = 2\pi R. \quad (5.3)$$

The mean handoff rate per calling mobile μ_h can be approximated by μ_b [19], i.e.,

$$\mu_h \approx \frac{E[V]L}{\pi A} = \frac{2E[V]}{\pi R}. \quad (5.4)$$

Thus, the mean call departure rate due to terminations from call completions and handoffs is

$$\mu_t = \mu + \mu_h \approx \mu + \frac{2E[V]}{\pi R}. \quad (5.5)$$

It is shown in [20] that (5.5) provides a good approximation of the mean call departure rate for Mobility Model A and B.

5.2 Handoff Model

The simulation model described in Section 4.1 is used to examine the performances of the proposed DCA scheme and some previously studied schemes. For the simulation involving handoffs, the cell boundary is assumed to be circular. An MS in cell x is only handed off to a neighboring cell when the distance between the MS and the BS of cell x exceeds R . When the MS reaches the system boundary, it is assumed to stay in the same cell until the call is terminated. In practice, the MS location and the link measurement between the MS and the BS are frequently updated and the handoff is performed immediately when the measurement falls below an acceptable threshold level. However, the frequent MS location updates will result in increased execution time. To simplify the simulation, the MS location is only updated whenever a new call arrives in a cell.

5.3 FCA Blocking Probability with Mobility Model A and B

In this section, we approximate the total call blocking probability P_b for the FCA scheme to investigate the characteristics of Mobility Model A and B. The average number of handoffs per successful call is obtained from simulations to approximate P_b for the FCA scheme with these

mobility models¹. Figure 5.2 shows a Markov chain state diagram for the FCA scheme with handoffs.

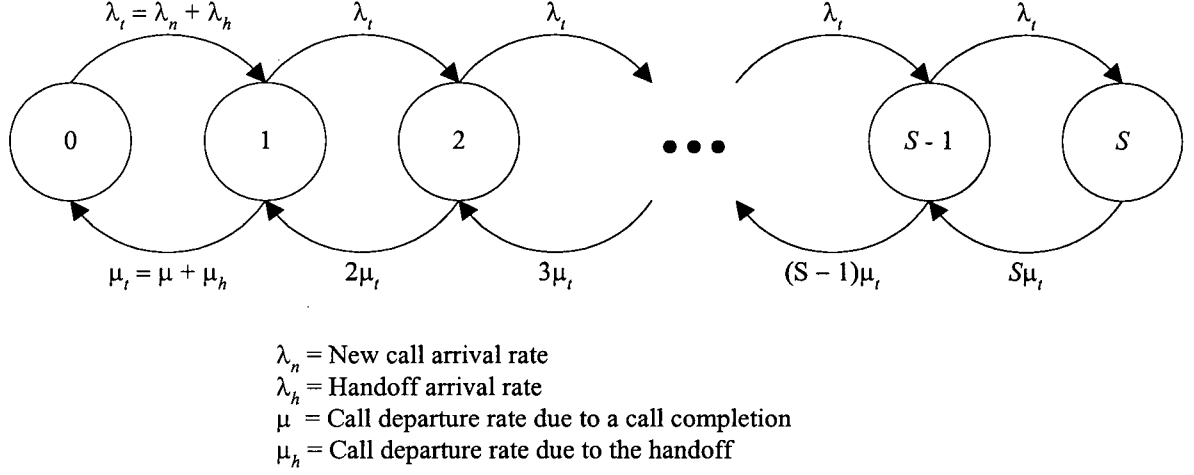


Figure 5.2: Markov Chain State Diagram for FCA Scheme.

In Figure 5.2, the number associated with each state corresponds to the number of channels used in the cell where each cell has S nominal channels. The blocking probability of call channel requests (i.e., new call arrival or handoff arrival), P_b' , for the FCA scheme can be obtained using the Erlang B formula [2] which is given in (2.6). The approximation of mean handoff rate of calling mobile μ_h is shown in (5.1). In [19], the handoff arrival rate λ_h is given as a function of μ_h and the expected number of calls in a cell as

$$\lambda_h = E[\text{calls}] \mu_h \quad (5.6)$$

where $E[\text{calls}]$ is given by

¹ A new call is successful if it is not blocked and all required handoffs are successful.

$$E[\text{calls}] = \sum_{i=1}^S i p_i. \quad (5.7)$$

The probability p_i that i channels are occupied in the cell is

$$p_i = \text{prob}\{i \text{ channels are busy}\} = \left(\frac{\lambda^i}{i! \mu_i} \right) p_0 \quad (5.8)$$

where p_0 is given by

$$p_0 = \frac{1}{\sum_{i=0}^S \frac{\lambda_i^i}{i! \mu_i}}. \quad (5.9)$$

Given that λ_n , μ , and μ_h , λ_h is solved iteratively using (2.6, 5.6 to 5.9) to calculate the blocking probability for the FCA scheme. Figure 5.3 shows a flowchart for approximating λ_h and P_b' . In (5.5), the mean handoff rate assumes that when an MS leaves its current cell, it goes to one of its 6 neighboring cells. In the simulation, a 49 hexagonal cell network is used so that some of the cells may not have 6 neighboring cells. As shown in Figure 4.1, the number of cells with 2, 3, 4, and 6 neighboring cells are 2, 2, 20, and 25 respectively. To calculate the average handoff rate per cell, we adjust the mean handoff rate using the average number, N_C , of the neighboring cells per cell which is as follows

$$N_C = \frac{1}{49}(2 \times 2 + 2 \times 3 + 20 \times 4 + 25 \times 6) = 4\frac{44}{49} \text{ cells}. \quad (5.10)$$

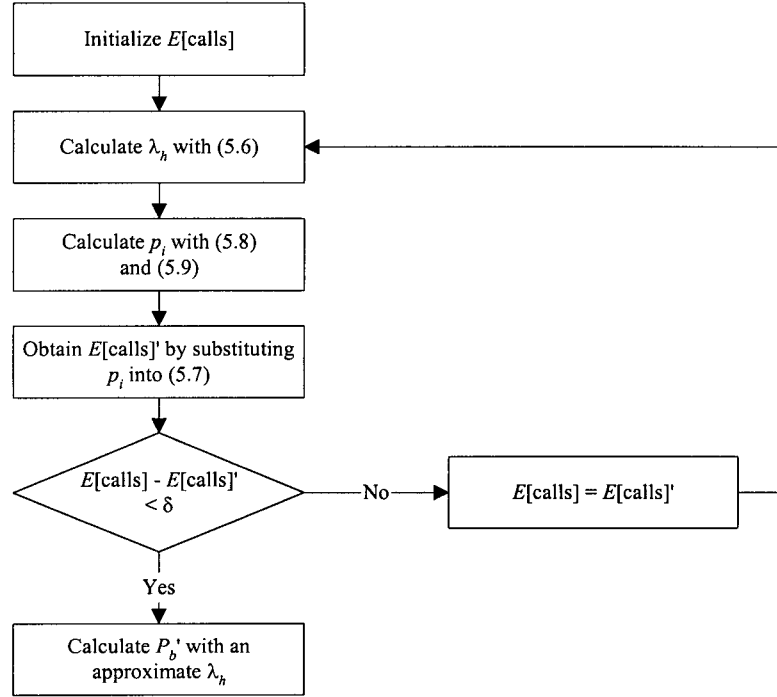


Figure 5.3: Approximation of Handoff Arrival Rate λ_h and Blocking Probability of Call Channel Requests P_b' .

The adjusted mean handoff rate, μ_h' , is given by

$$\mu_h' = \frac{N_C}{6} \left(\frac{2E[V]}{\pi R} \right) = \frac{E[V]N_C}{3\pi R}. \quad (5.11)$$

In Figure 5.3, the adjusted mean handoff rate is used to estimate the handoff arrival rate with (5.6). The value of δ is chosen to be 10^{-9} . The Erlang B formula in (2.6) assumes that call requests are memoryless and the inter-arrival times of call requests are independent of each other. Moreover, new call and handoff arrival rates are assumed to be a Poisson process. On the other hand, handoff arrival rates for both mobility models are not a Poisson process and are dependent on the speed and direction of the calling MS. Hence, we approximate blocking probabilities for

both mobility models with the average channel requests of calling mobiles due to new call arrivals and handoffs. The average number of channel requests for a new call arrival is 1. Let $h(V)$ denote the average number of handoffs per successful call. The average number of channel requests for each calling mobile is given by

$$E[\text{channel requests for each calling mobile}] = 1 + h(V). \quad (5.12)$$

The average number of handoffs per successful call $h(V)$ was obtained from simulations. For the simulation, the MS speed V is uniformly distributed in $(0, V_{\max})$ and the cell radius R is chosen to be 1 km. Figures 5.4 and 5.5 show the average number of handoffs per successful call as a function of MS maximum speed. In this chapter, the 99% confidence interval associated with each simulation point is within $\pm 5\%$ of the average values plotted.

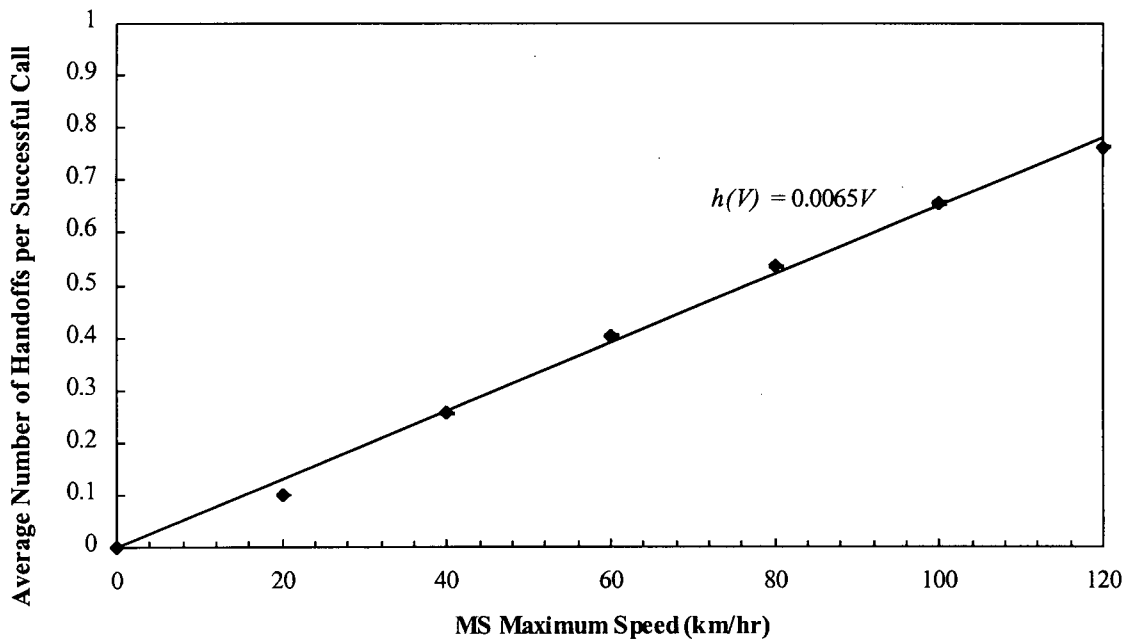


Figure 5.4: Average Number of Handoffs per Successful Call as a Function of MS Maximum Speed with Mobility Model A.

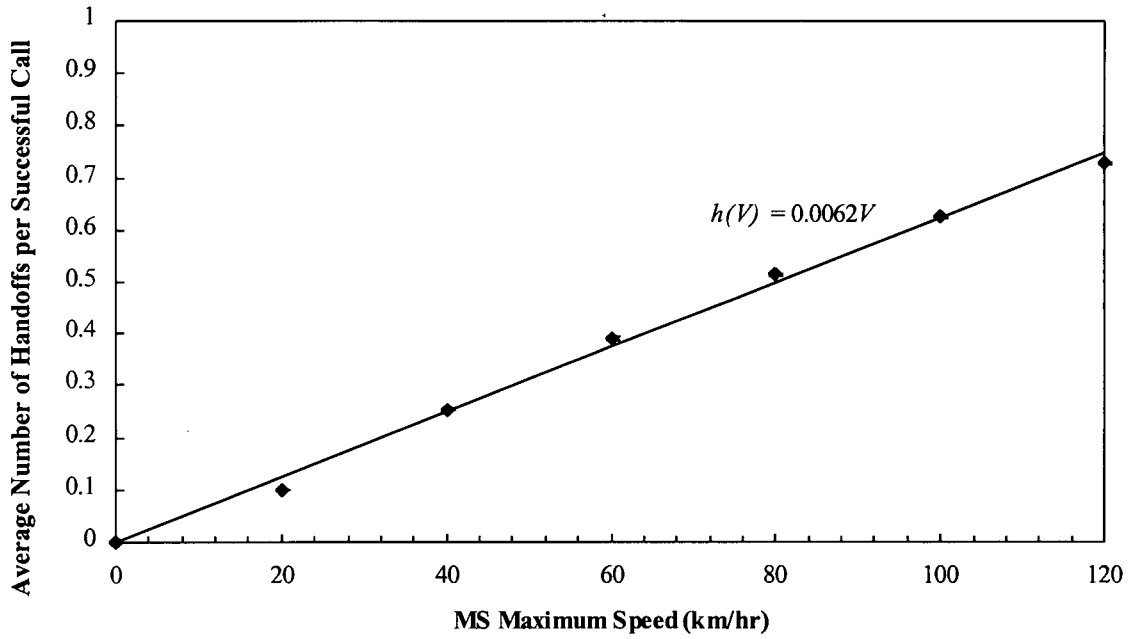


Figure 5.5: Average Number of Handoffs per Successful Call as a Function of MS Maximum Speed with Mobility Model B.

As shown in Figures 5.4 and 5.5, the average number of handoffs per successful call increases with the MS maximum speed, V_{\max} , where the MS speed is uniformly distributed in $(0, V_{\max})$. The average number of handoffs per successful call for Mobility Model A and B with no handoff failures are given by

$$h(V) = \begin{cases} 0.0065 V & \text{for Mobility Model A and } P_{bh} = 0 \\ 0.0062 V & \text{for Mobility Model B and } P_{bh} = 0. \end{cases} \quad (5.13)$$

The average number of handoffs per successful call for Mobility Model A is slightly higher than for Mobility Model B. The slight difference in the average number of handoffs per successful call may be caused by the regeneration of the MS speed and direction in Mobility Model B when the MS crosses a cell boundary. Given the average number of handoffs per successful call function

$h(V)$ for Mobility Model A and B, the total call blocking probability, P_b , for the FCA scheme is given by

$$\begin{aligned}
 P_b &= 1 - \text{prob}\{\text{new call arrival is not blocked}\} \cdot \text{prob}\{\text{no handoff failure}\} \\
 &= 1 - (1 - P_b')^1 \cdot (1 - P_b')^{h(V)} \\
 &= 1 - (1 - P_b')^{1 + h(V)}.
 \end{aligned} \tag{5.14}$$

The approximate total call blocking probability obtained by (5.13) and (5.14) are compared with the simulation results. The handoff model described in Section 5.2 is used for examining the performance of the FCA scheme. Figures 5.6 and 5.7 show approximate and simulation results of the total call blocking probability for the FCA scheme as a function of MS maximum speed ranging from 0 to 120 km/hr. The approximate and simulation results are in good agreement with a difference between approximate and simulation results of at most $\pm 7\%$.

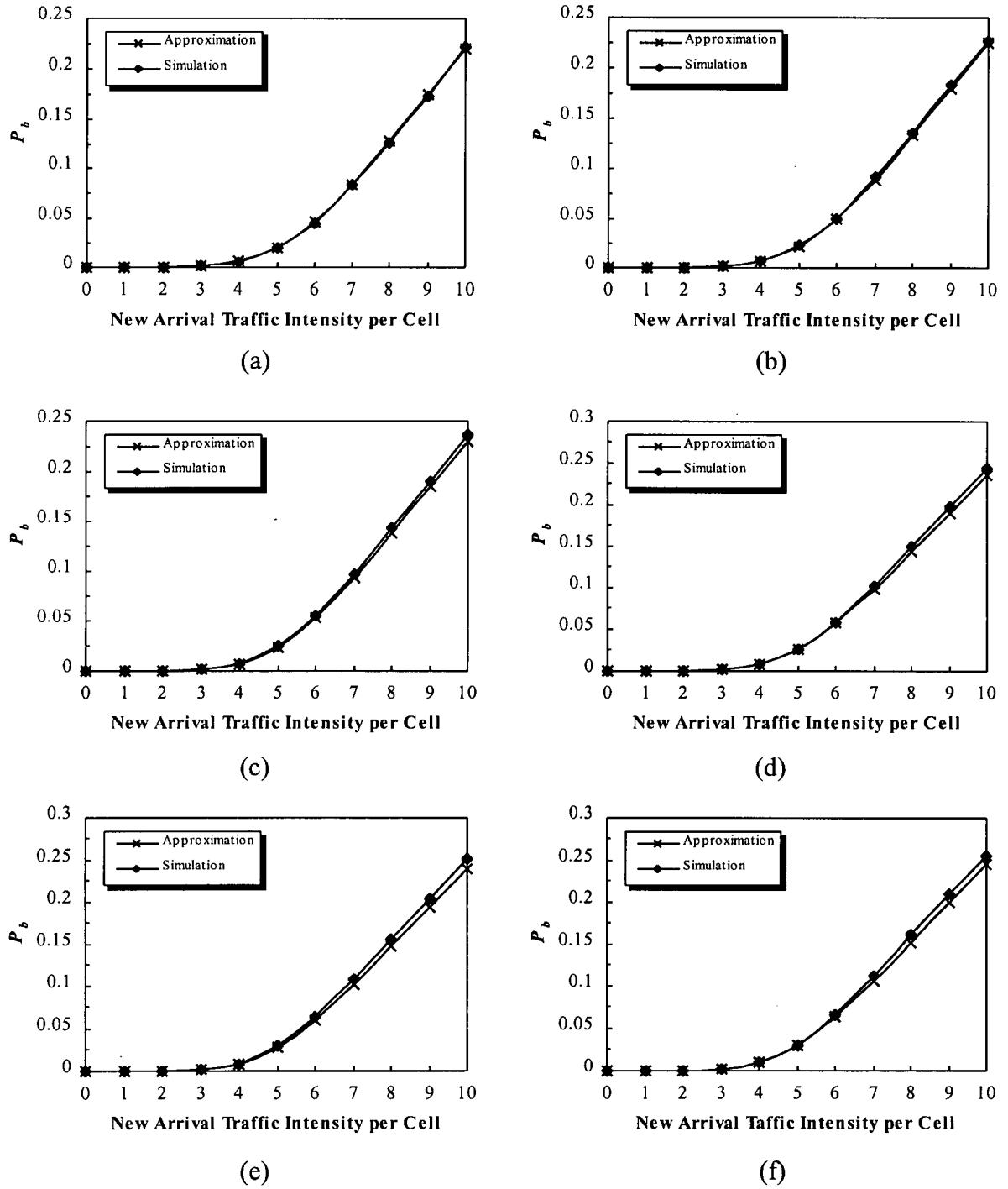


Figure 5.6: Approximate and Simulation Results for Total Call Blocking Probability, P_b , for the FCA Scheme (averaged over 49 cells) with Mobility Model A. (a) $V_{\max} = 20$ km/hr, (b) $V_{\max} = 40$ km/hr, (c) $V_{\max} = 60$ km/hr, (d) $V_{\max} = 80$ km/hr, (e) $V_{\max} = 100$ km/hr, (f) $V_{\max} = 120$ km/hr.

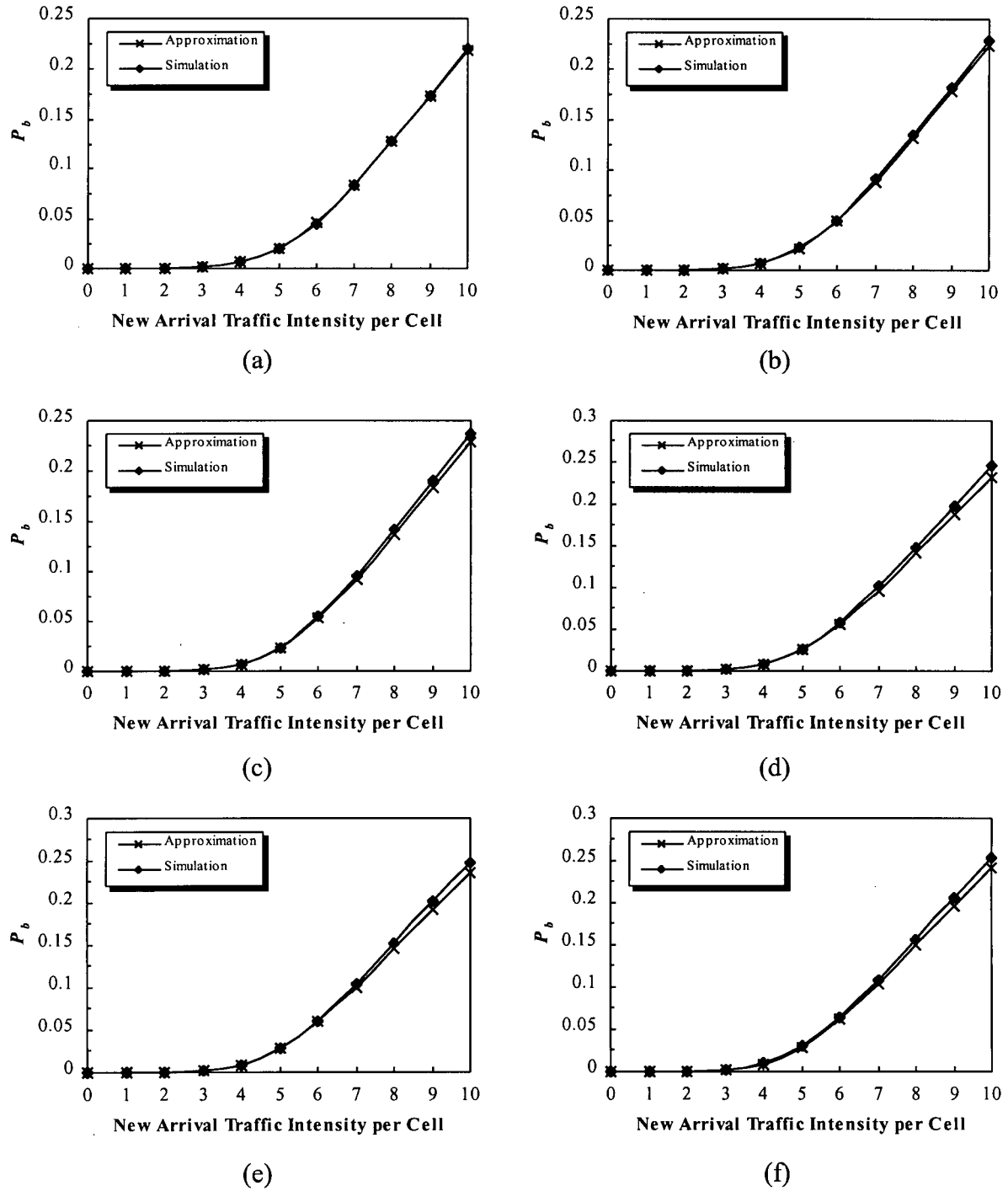


Figure 5.7: Approximate and Simulation Results for Total Call Blocking Probability, P_b , for the FCA Scheme (averaged over 49 cells) with Mobility Model B. (a) $V_{\max} = 20$ km/hr, (b) $V_{\max} = 40$ km/hr, (c) $V_{\max} = 60$ km/hr, (d) $V_{\max} = 80$ km/hr, (e) $V_{\max} = 100$ km/hr, (f) $V_{\max} = 120$ km/hr.

5.4 Results and Discussions

In this section, we study the performance of the proposed DCA scheme with two mobility models: Mobility Model A and B. Simulation results of the proposed scheme with mobility are presented in uniform and non-uniform traffic distributions and then compared to some previously studied channel assignment schemes.

5.4.1 Uniform Traffic Distribution

The handoff management of a channel assignment scheme impacts the performance of the cellular system. Handoff operations must be performed successfully and as infrequently as possible, and be imperceptible to mobile users. In this section, the simulation results of the proposed DCA scheme and the comparison between the proposed scheme and some previously studied channel assignment schemes with mobility and uniform traffic distribution are presented. The two mobility models described in Section 5.1 are used to examine the capacity and reliability of mobile services in terms of the new call blocking probability, the handoff blocking probability, the dropped call probability, and the total call blocking probability.

The new call arrival process is Poisson and the call duration is exponentially distributed with a mean of 2 minutes. For the simulation, the cell radius is 1 km and a call is randomly generated in one of the 49 cells with a uniform traffic distribution where its speed and direction are uniformly distributed in $(0, V_{\max})$ and $(0, 2\pi)$ respectively. Figures 5.8 to 5.15 show the results of the new call blocking probability, the handoff blocking probability, the dropped call probability, and the total call blocking probability of the central 9 cells and all 49 cells with

Mobility Model A where the MS maximum speeds are 60 and 120 km/hr respectively.

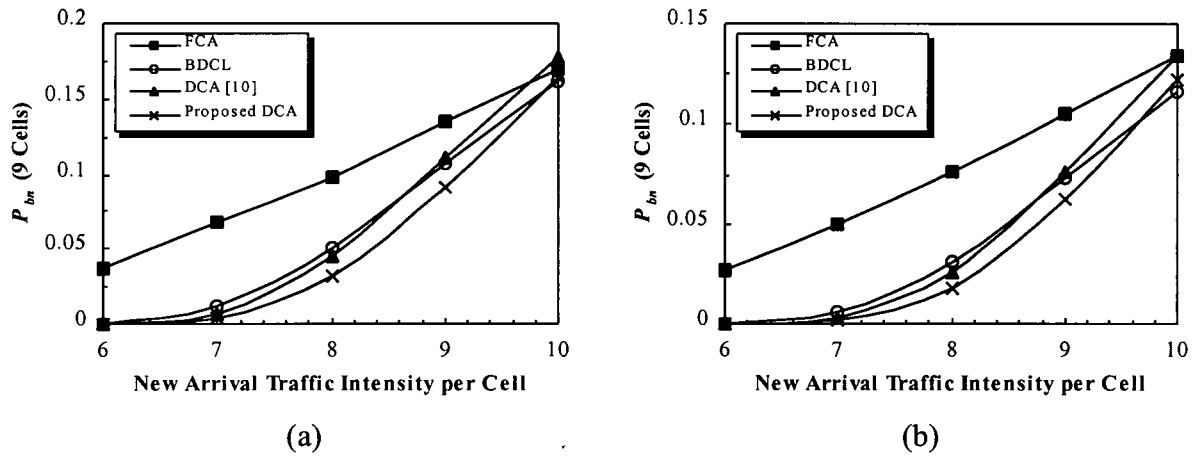


Figure 5.8: New Call Blocking Probability, P_{bn} , (averaged over central 9 cells) with Mobility Model A. (a) $V_{max} = 60$ km/hr, (b) $V_{max} = 120$ km/hr.

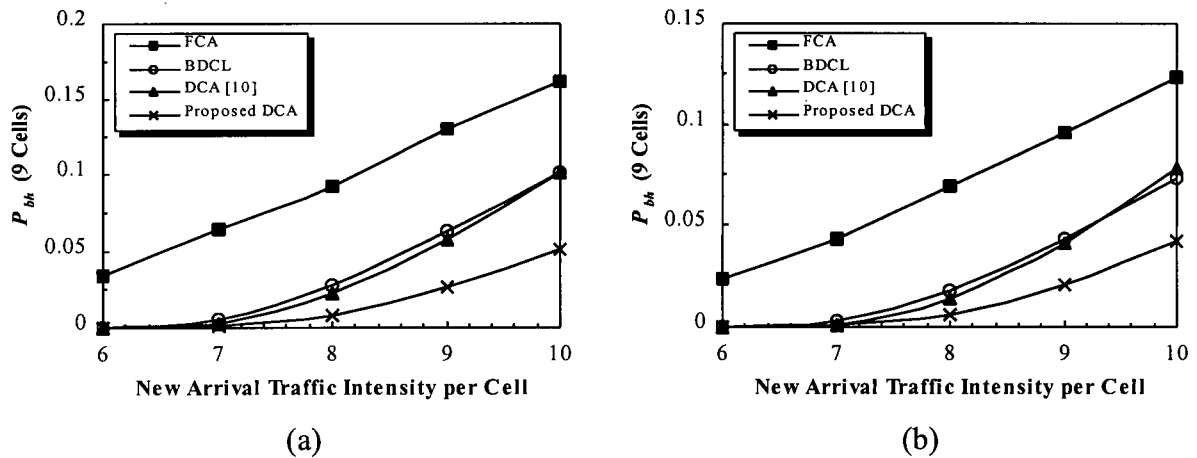
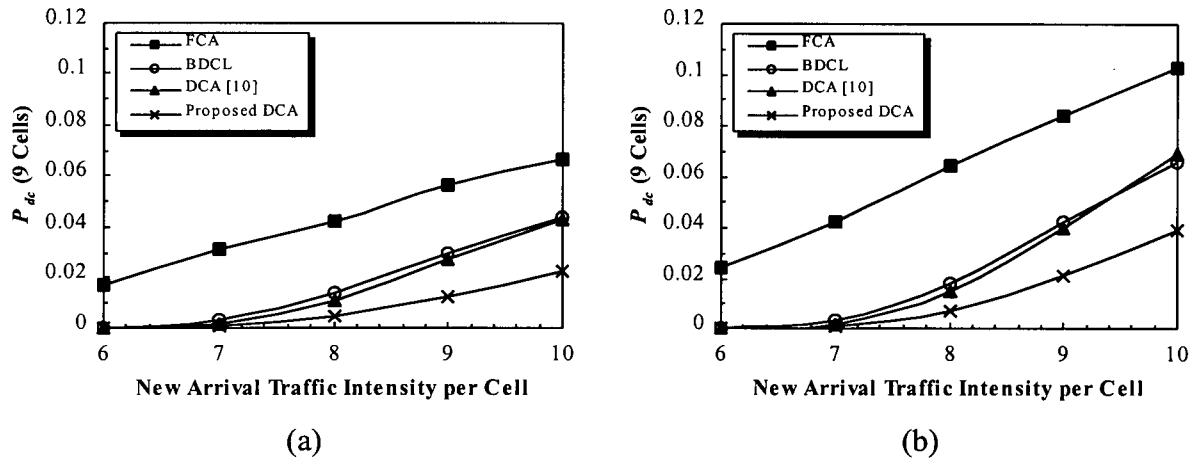
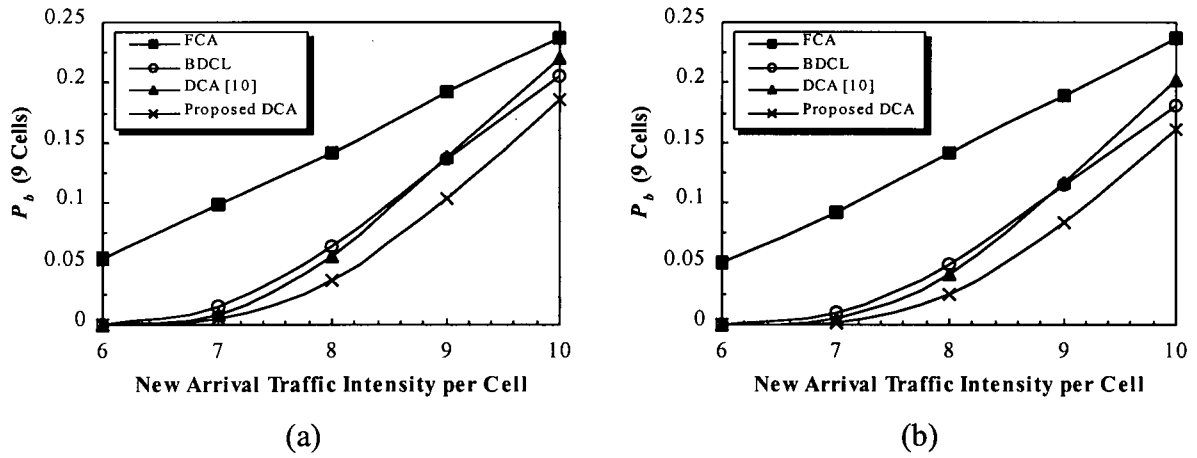


Figure 5.9: Handoff Blocking Probability, P_{bh} , (averaged over central 9 cells) with Mobility Model A. (a) $V_{max} = 60$ km/hr, (b) $V_{max} = 120$ km/hr.

Figure 5.10: Dropped Call Probability, P_{dc} , (averaged over central 9 cells) with Mobility ModelA. (a) $V_{\max} = 60$ km/hr, (b) $V_{\max} = 120$ km/hr.Figure 5.11: Total Call Blocking Probability, P_b , (averaged over central 9 cells) with MobilityModel A. (a) $V_{\max} = 60$ km/hr, (b) $V_{\max} = 120$ km/hr.

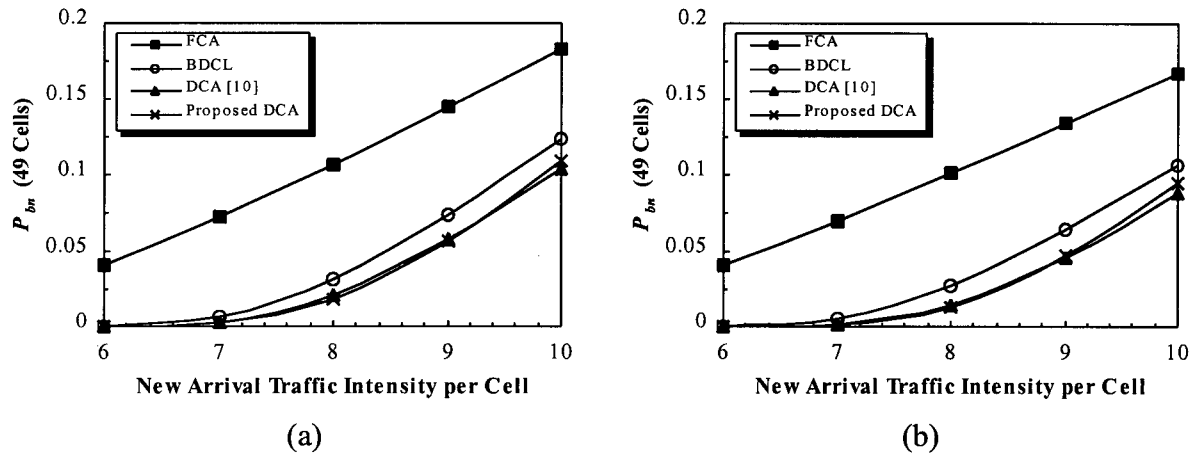


Figure 5.12: New Call Blocking Probability, P_{bn} , (averaged over 49 cells) with Mobility Model A. (a) $V_{\max} = 60$ km/hr, (b) $V_{\max} = 120$ km/hr.

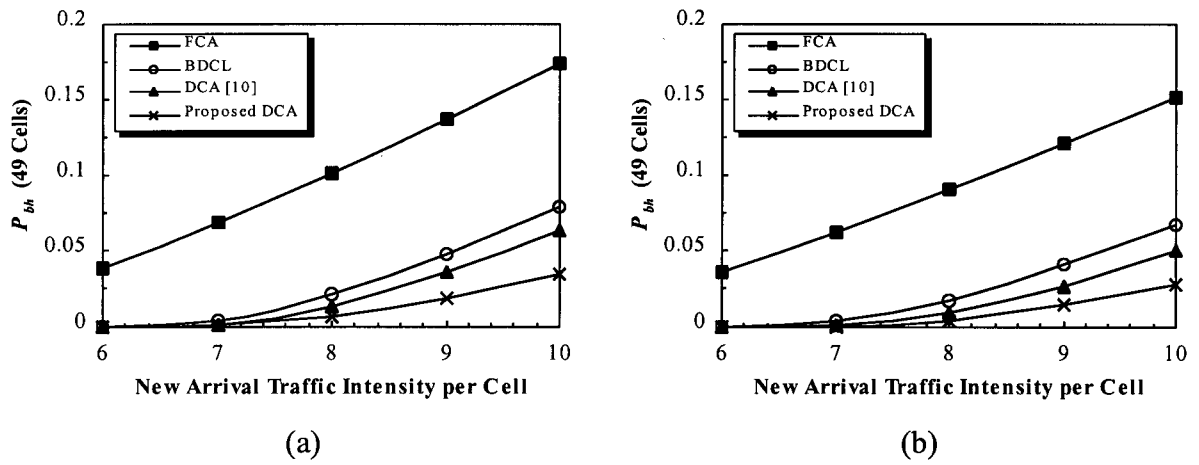


Figure 5.13: Handoff Blocking Probability, P_{bh} , (averaged over 49 cells) with Mobility Model A. (a) $V_{\max} = 60$ km/hr, (b) $V_{\max} = 120$ km/hr.

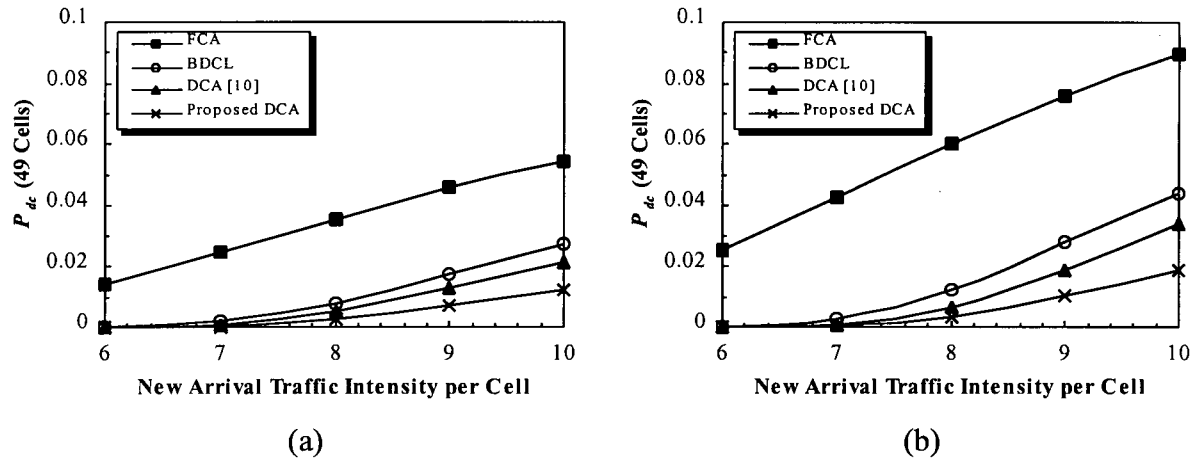
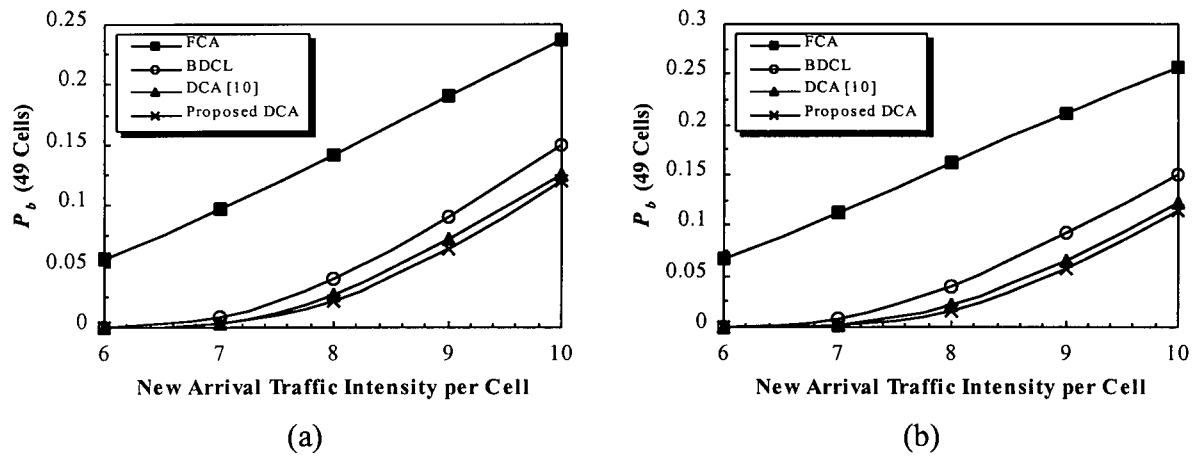
Figure 5.14: Dropped Call Probability, P_{dc} , (averaged over 49 cells) with Mobility Model A.(a) $V_{\max} = 60$ km/hr, (b) $V_{\max} = 120$ km/hr.Figure 5.15: Total Call Blocking Probability, P_b , (averaged over 49 cells) with Mobility Model A.(a) $V_{\max} = 60$ km/hr, (b) $V_{\max} = 120$ km/hr.

Figure 5.8 shows the proposed DCA scheme performs better in the new call blocking probability of the central 9 cells than other channel assignment schemes when the new arrival traffic intensity is less than 10. At a traffic intensity of 10, the new call blocking probability for the proposed scheme at 60 and 120 km/hr are 16.4% and 12.2% respectively which are slightly

higher than the BDCL scheme (16.1% and 11.6%). In Figure 5.9 and 5.10, the proposed DCA scheme always gives the lowest handoff blocking probability and dropped call probability for the central 9 cells, followed by the DCA [10], the BDCL and the FCA schemes. Handoff blocking and dropped call probabilities for the BDCL and the DCA [10] schemes (at both 60 and 120 km/hr) are approximately two times higher than the proposed scheme. The higher dropped call probability results in a lower blocking probability of new call attempts since more calls are dropped. Therefore, the BDCL scheme performs slightly better in terms of the new call blocking probability than the proposed scheme. The simulation results presented in Figures 5.9 and 5.10 show that the channel borrowing and re-assigning strategy provides lower handoff blocking and dropped call probabilities. As shown in Figure 5.11, the proposed scheme gives the lowest total call blocking probability of the central 9 cells.

Figures 5.12 to 5.15 illustrate the new call blocking probability, the handoff blocking probability, the dropped call probability, and the total call blocking probability of all 49 cells with Mobility Model A at MS maximum speeds of 60 and 120 km/hr respectively. As presented in Figures 5.12 to 5.14, the new call blocking probability of the proposed DCA scheme is slightly worse than the DCA [10] scheme but it has the lower handoff blocking probability and dropped call probability. The simulation results presented in Figure 5.14 show that the dropped call probability of all 49 cells is increased as the MS maximum speed increases. Because the new call blocking probability is correlated with the handoff blocking probability and the dropped call probability, the increase in handoff failures can reduce the number of new calls blocked. Figure 5.15 indicates that the proposed DCA scheme always gives the lowest total call blocking probability. In Figures 5.11 and 5.15, the total call blocking probabilities of all four channel assignment schemes are lower at the higher MS maximum speed.

To study the performance of the channel assignment schemes, we simulate these schemes with Mobility Model B at MS maximum speeds of 60 and 120 km/hr respectively. The simulation results for Mobility Model B of the new call blocking probability, the handoff blocking probability, the dropped call probability, and the total call blocking probability of the central 9 cells and all 49 cells are presented in Figures 5.16 to 5.23.

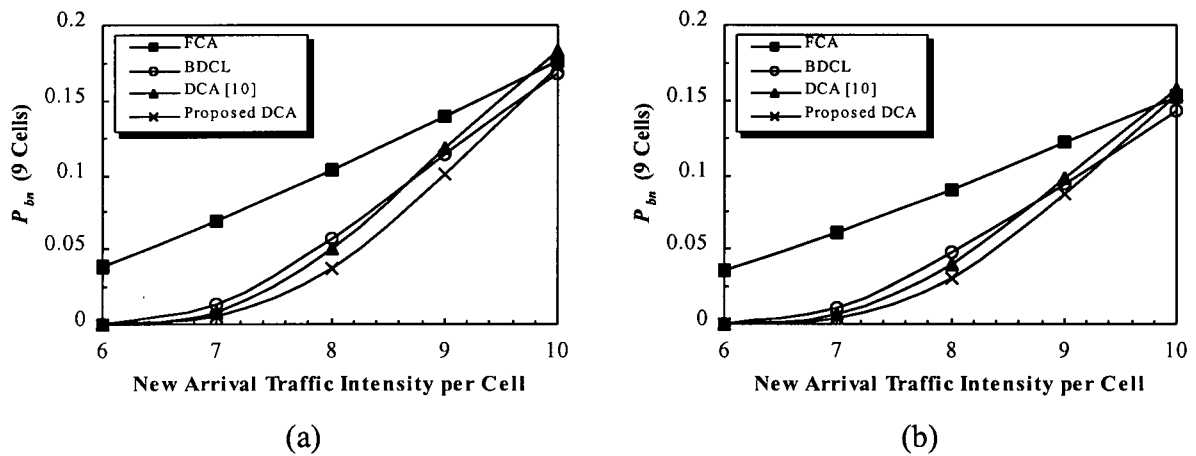


Figure 5.16: New Call Blocking Probability, P_{bn} , (averaged over central 9 cells) with Mobility Model B. (a) $V_{\max} = 60$ km/hr, (b) $V_{\max} = 120$ km/hr.

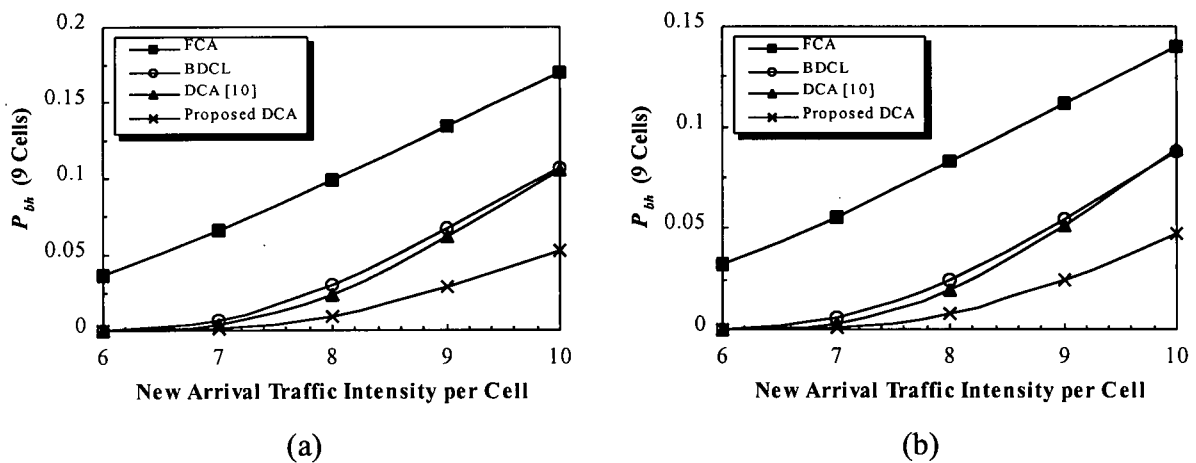


Figure 5.17: Handoff Blocking Probability, P_{bh} , (averaged over central 9 cells) with Mobility Model B. (a) $V_{\max} = 60$ km/hr, (b) $V_{\max} = 120$ km/hr.

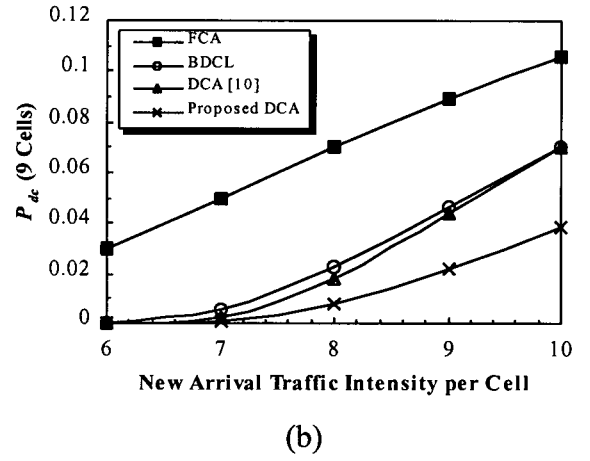
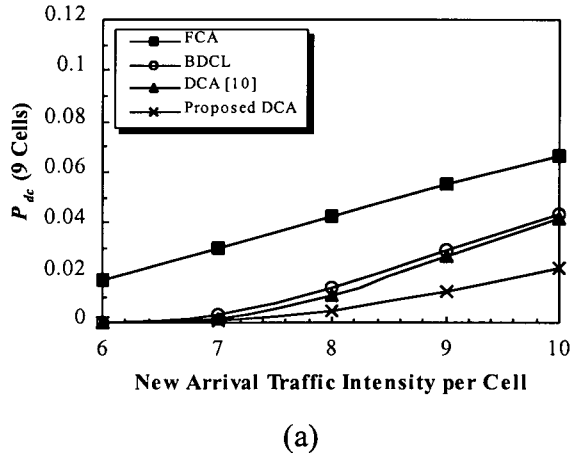


Figure 5.18: Dropped Call Probability, P_{dc} , (averaged over central 9 cells) with Mobility Model B. (a) $V_{max} = 60$ km/hr, (b) $V_{max} = 120$ km/hr.

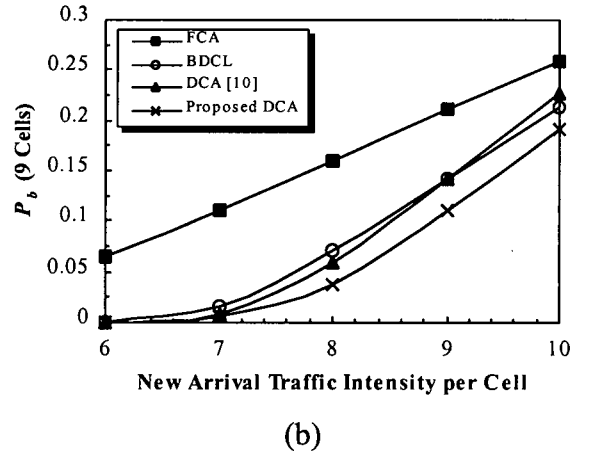
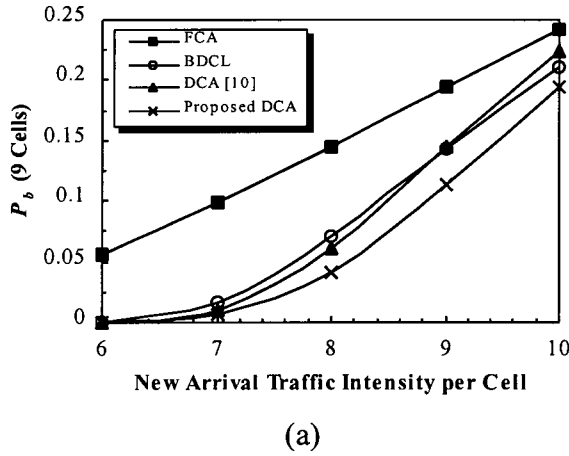


Figure 5.19: Total Call Blocking Probability, P_b , (averaged over central 9 cells) with Mobility Model B. (a) $V_{max} = 60$ km/hr, (b) $V_{max} = 120$ km/hr.

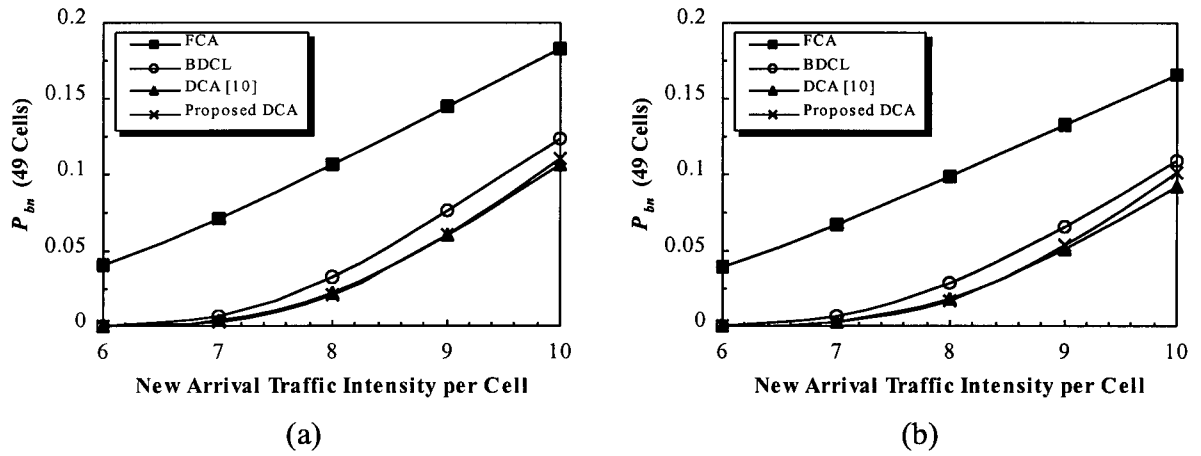


Figure 5.20: New Call Blocking Probability, P_{bn} , (averaged over 49 cells) with Mobility Model B. (a) $V_{\max} = 60$ km/hr, (b) $V_{\max} = 120$ km/hr.

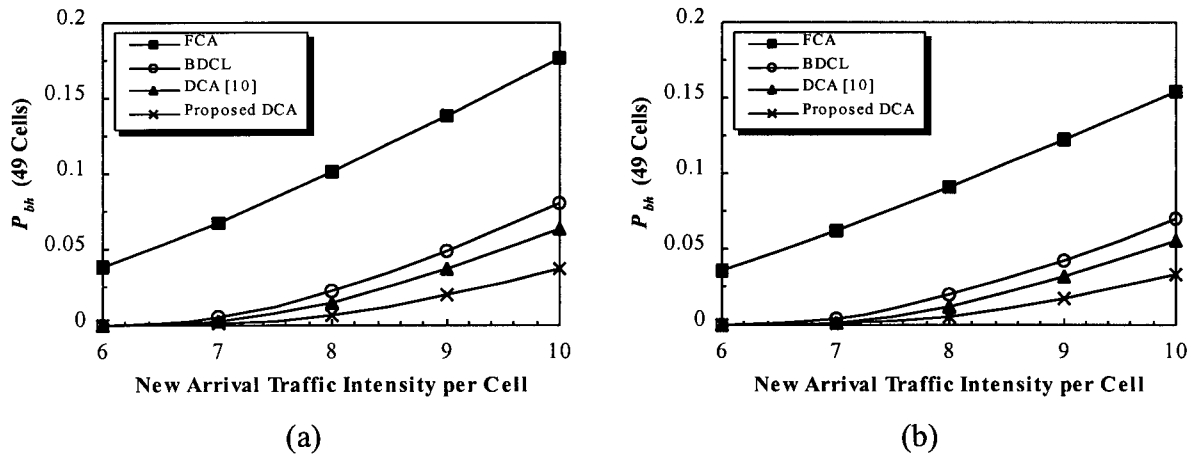
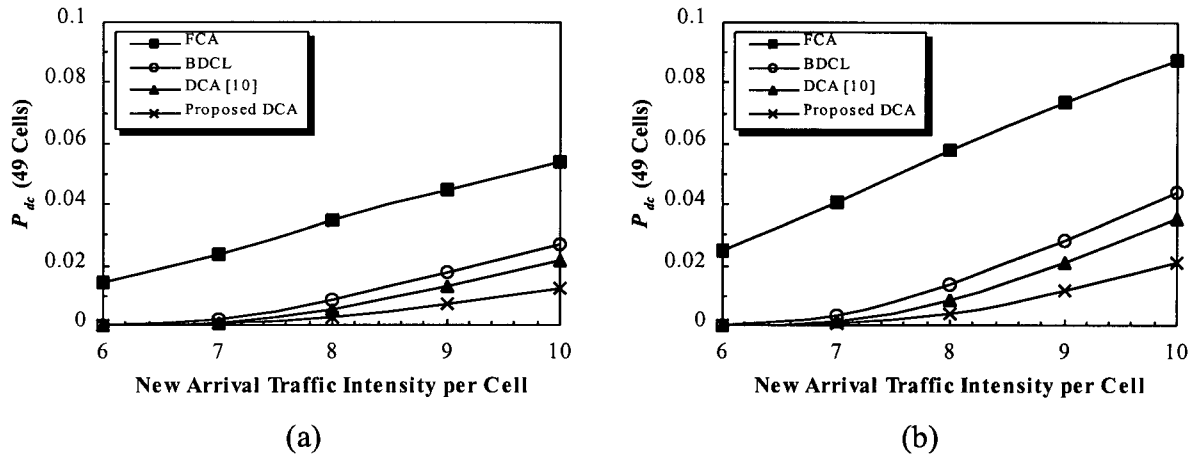
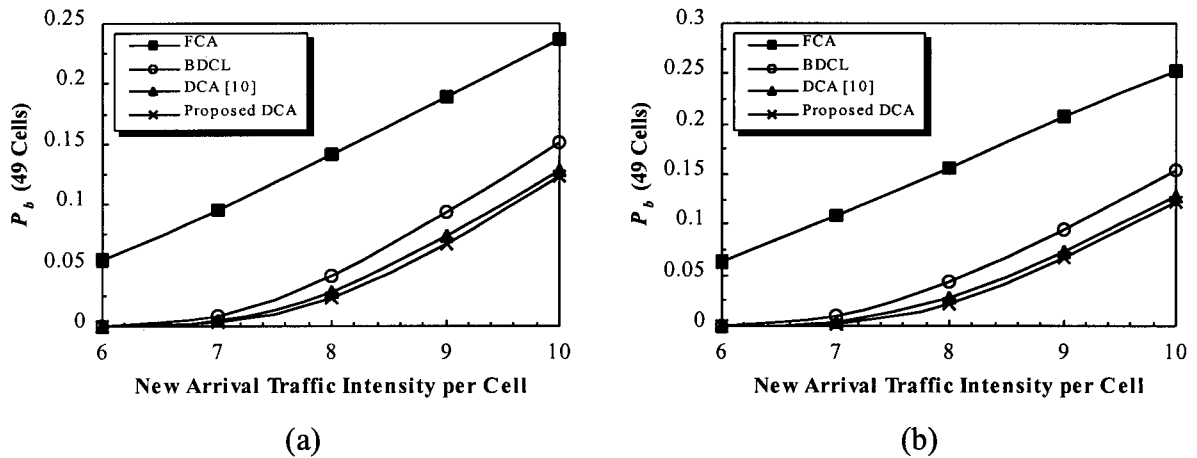


Figure 5.21: Handoff Blocking Probability, P_{bh} , (averaged over 49 cells) with Mobility Model B. (a) $V_{\max} = 60$ km/hr, (b) $V_{\max} = 120$ km/hr.

Figure 5.22: Dropped Call Probability, P_{dc} , (averaged over 49 cells) with Mobility Model B.(a) $V_{\max} = 60$ km/hr, (b) $V_{\max} = 120$ km/hr.Figure 5.23: Total Call Blocking Probability, P_b , (average over 49 cells) with Mobility Model B.(a) $V_{\max} = 60$ km/hr, (b) $V_{\max} = 120$ km/hr.

Figures 5.16 to 5.23 show that the simulation results with Mobility Model B are similar to the results with Mobility Model A. As shown in Figures 5.16 and 5.18, the new call blocking probability of the BDCL scheme for the central 9 cells is slightly lower than the proposed DCA scheme because the BDCL scheme has a higher dropped call probability. The proposed scheme

always gives the lowest handoff blocking probability and total call blocking probability of the central 9 cells and all 49 cells followed by the DCA [10], the BDCL, and the FCA schemes. With the channel borrowing and re-assigning strategy, the proposed scheme can significantly reduce the number of handoff failures so that the good quality mobile services are provided. From Figure 5.22, it can be seen that, as in the case of Mobility Model B, an increase in the MS maximum speed increases the dropped call probability. Figures 5.8 to 5.23 demonstrate that the new call blocking probability and the handoff blocking probability with Mobility Model A are slightly lower than with Mobility Model B. The slight difference between these two mobility models may be caused by the regeneration of the MS direction and speed when the MS crosses a cell boundary in Mobility Model B.

The BS has a circular signal coverage area and the handoff operation is only performed when the distance between the MS and the BS is greater than R . In our simulation, we assume that the cell boundary is a circle with a radius of R . As the circular signal coverage area is slightly larger than the hexagonal area, we also simulated the channel assignment schemes with the hexagonal cell boundary. The simulation results demonstrate that the difference between circular and hexagonal cell boundaries in terms of blocking probabilities are at most $\pm 5\%$. Because of the small difference in results between circular and hexagonal cell boundaries, the cell boundary is assumed to be a circle of radius R in order to simplify the computer simulations.

5.4.2 Call Blocking Distribution

In this section, computer simulations are performed with three different MS maximum

speeds to study the effect of the MS maximum speed on the call blocking distributions in different tier cells (See Figure 4.8). Figures 5.24 to 5.26 show the simulation results of proposed DCA scheme with Mobility Model A. The simulation results of the proposed DCA scheme are examined with a uniform traffic distribution at MS maximum speeds of 20, 60, and 120 km/hr respectively.

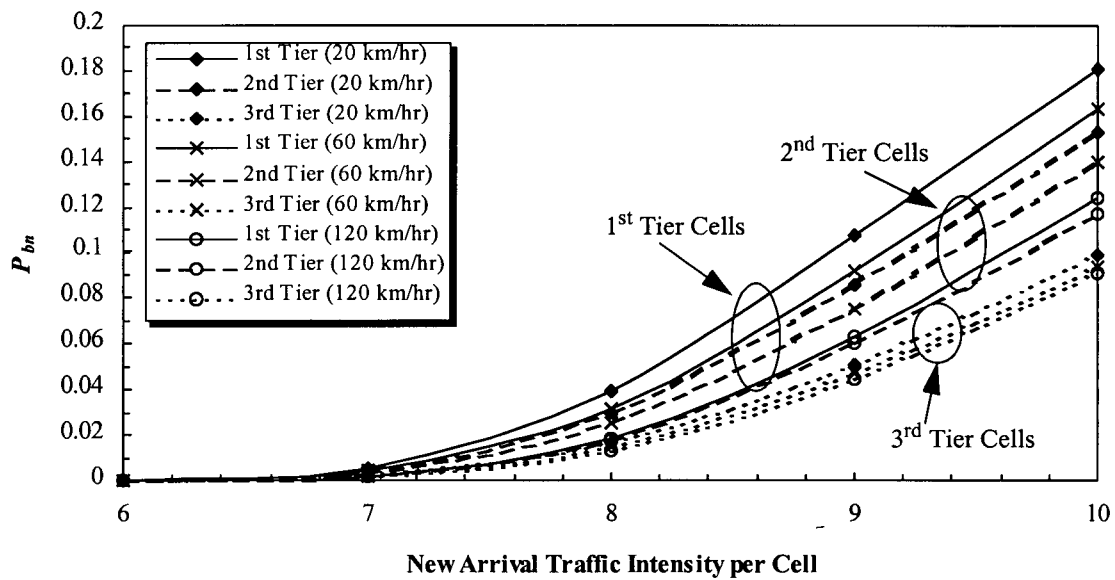


Figure 5.24: New Call Blocking Probability, P_{bn} , of Three Tier Cells for the Proposed DCA Scheme with Mobility Model A and Three Different MS Maximum Speeds ($V_{\max} = 20, 60$, and 120 km/hr).

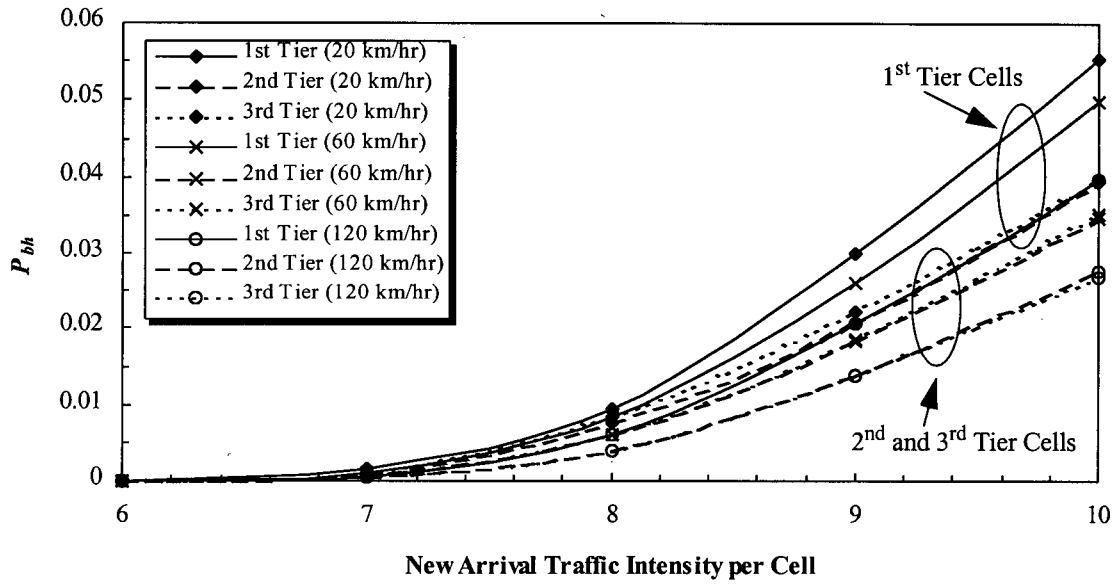


Figure 5.25: Handoff Blocking Probability, P_{bh} , of Three Tier Cells for the Proposed DCA Scheme with Mobility Model A and Three Different MS Maximum Speeds ($V_{\max} = 20, 60$, and 120 km/hr).

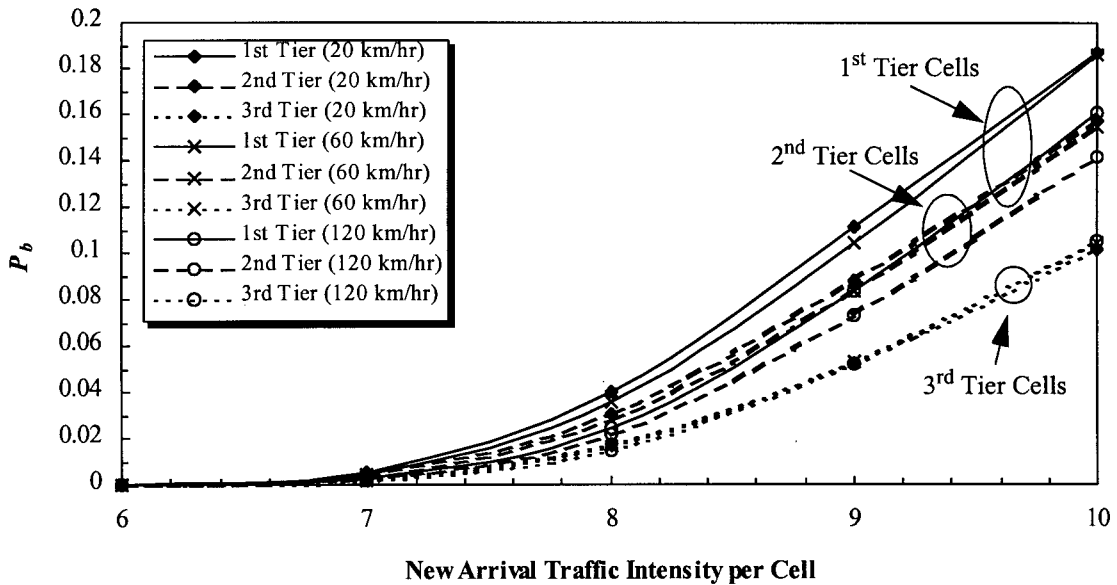


Figure 5.26: Total Call Blocking Probability, P_b , of Three Tier Cells for the Proposed DCA Scheme with Mobility Model A and Three Different MS Maximum Speeds ($V_{\max} = 20, 60$, and 120 km/hr).

As shown in Figures 5.24 to 5.26, the new call blocking probability, the handoff blocking probability, and the total call blocking probability for the first tier cells are the highest followed by the second and third tier cells. The simulation results indicate that the number of handoff attempts and handoff failures depend on the MS maximum speed. As the MS maximum speed increases, the blocking probabilities for the first and second tier cells are lowered because more calling MS's reach the system boundary thus resulting in a lower traffic in these cells. Figures 5.25 and 5.26 show the increase of the MS maximum speed does not affect the handoff blocking probability and the total call blocking probability for the third tier cells. In the 49 hexagonal cell network, the first tier cells with a complete set of interfering cells always give the highest blocking probabilities.

5.4.3 Non-uniform Traffic Distribution

In the cellular system, the traffic distribution within the coverage area is non-uniform and each cell may have different distribution of mobile users. In this section, we examine the effect of blocking probabilities with mobility models and non-uniform traffic distributions. The non-uniform traffic distribution pattern shown in Figure 4.10(a) is used to study the performances of the proposed DCA scheme and other channel assignment schemes. The blocking probabilities are measured in all 49 cells while the traffic rate for each cell is increased from 0 to 100 percent over the base load. The base load corresponds to an average call arrival rate per cell of 150 calls/hour (i.e., the new arrival traffic intensity per cell is 5). Furthermore, the MS speed is uniformly distributed in $(0, V_{\max})$ where $V_{\max} = 60$ km/hr. The simulation results for Mobility Model A and B are summarized in Figures 5.27 to 5.32.

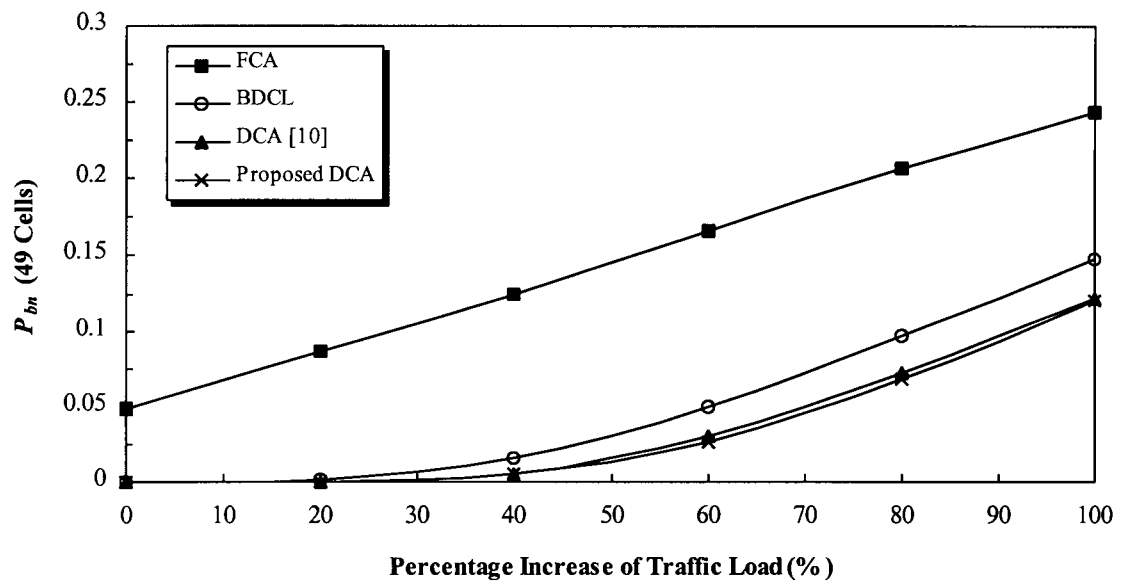


Figure 5.27: New Call Blocking Probability, P_{bn} , (averaged over 49 cells) with Mobility Model A ($V_{\max} = 60$ km/hr) and Non-uniform Traffic Distribution Pattern A.

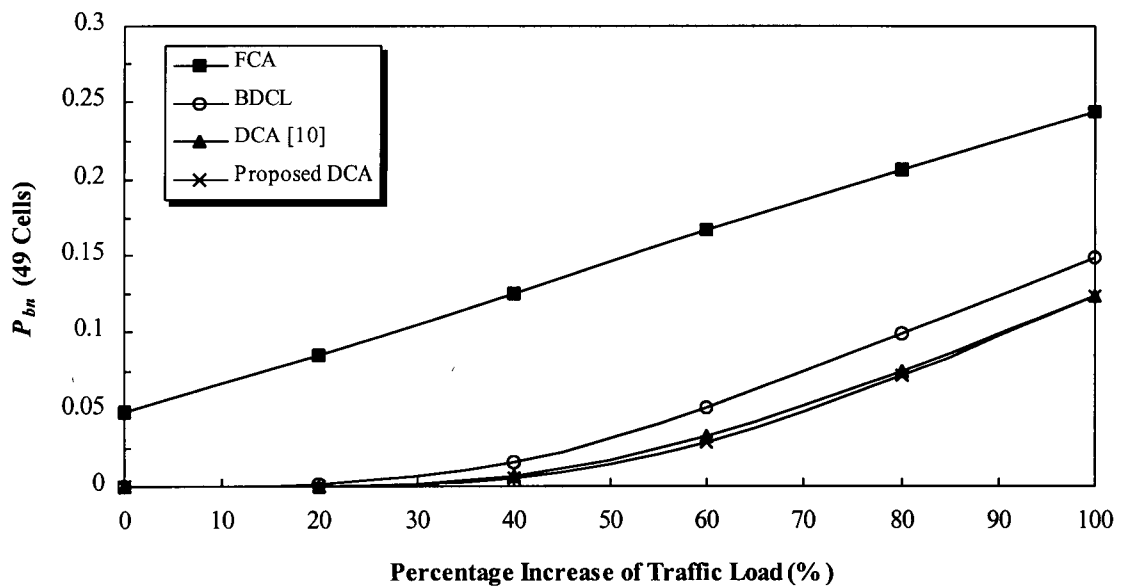


Figure 5.28: New Call Blocking Probability, P_{bn} , (averaged over 49 cells) with Mobility Model B ($V_{\max} = 60$ km/hr) and Non-uniform Traffic Distribution Pattern A.

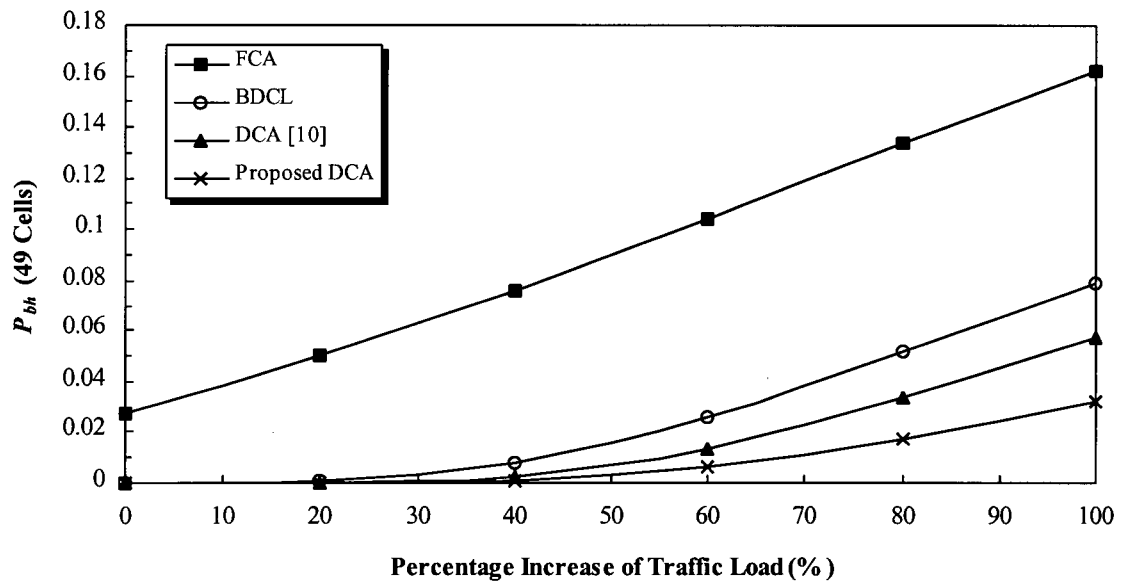


Figure 5.29: Handoff Blocking Probability, P_{bh} , (averaged over 49 cells) with Mobility Model A ($V_{\max} = 60$ km/hr) and Non-uniform Traffic Distribution Pattern A.

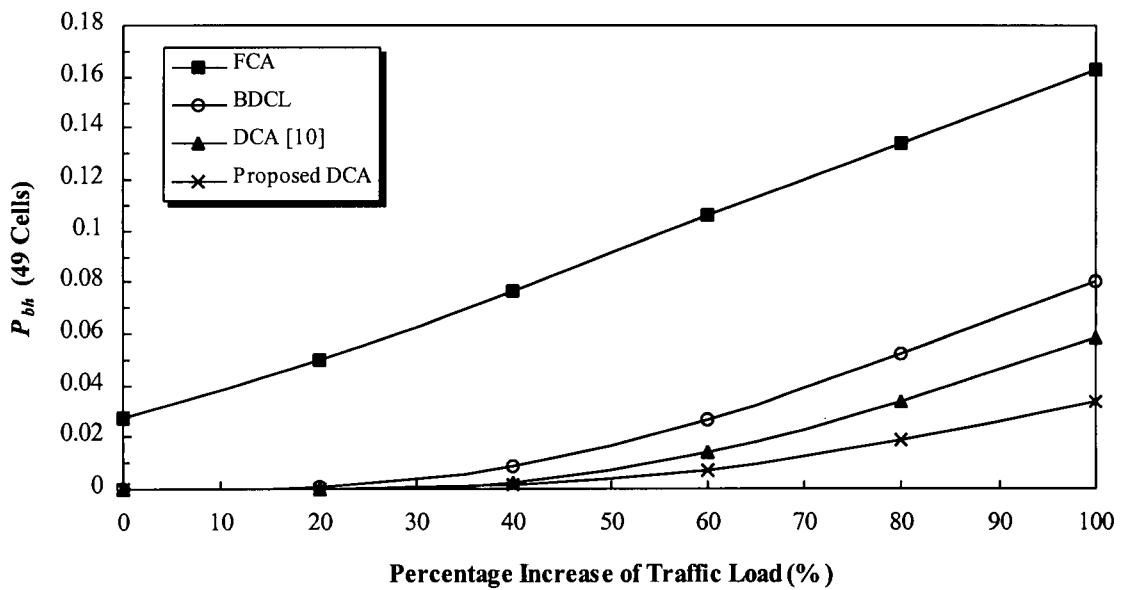


Figure 5.30: Handoff Blocking Probability, P_{bh} , (averaged over 49 cells) with Mobility Model B ($V_{\max} = 60$ km/hr) and Non-uniform Traffic Distribution Pattern A.

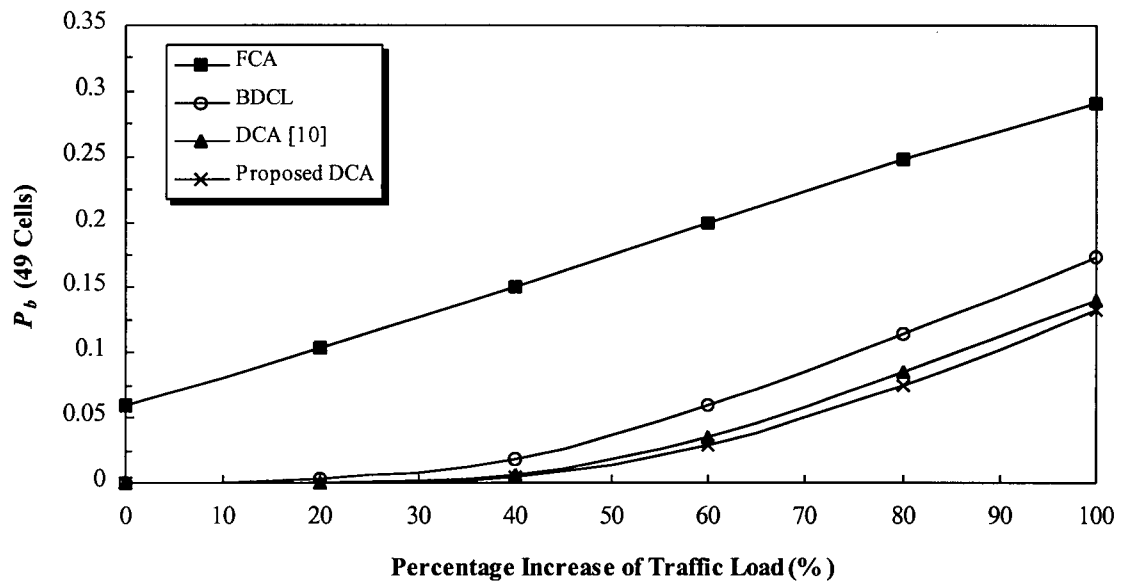


Figure 5.31: Total Call Blocking Probability, P_b , (averaged over 49 cells) with Mobility Model A ($V_{\max} = 60$ km/hr) and Non-uniform Traffic Distribution Pattern A.

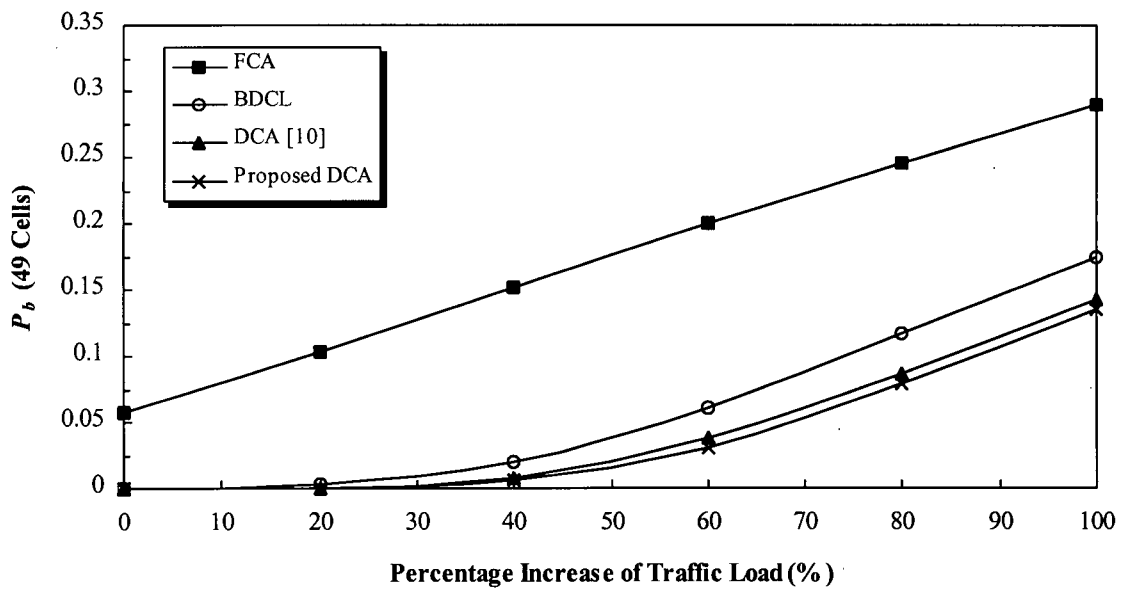


Figure 5.32: Total Call Blocking Probability, P_b , (averaged over 49 cells) with Mobility Model B ($V_{\max} = 60$ km/hr) and Non-uniform Traffic Distribution Pattern A.

With Mobility Model A and B, Figures 5.27 and 5.28 show that the new call blocking probability of the proposed DCA scheme is about the same as the DCA [10] scheme. Figures 5.29 and 5.30 illustrate that the lower handoff blocking probabilities are obtained by the proposed scheme. The simulation results presented in Figures 5.31 and 5.32 demonstrate the proposed scheme always gives the lowest total call blocking probability, followed by the DCA [10], the BDCL, and the FCA schemes.

5.5 Summary

Two mobility models were used to determine the performance of the channel assignment schemes in terms of the new call blocking probability and handoff blocking probability. An approximate method for calculating the total call blocking probability for the FCA scheme with these mobility models was also described. The approximate and simulation results are in good agreement with a difference of at most $\pm 7\%$. For both uniform and non-uniform traffic distributions, the proposed DCA has the lowest handoff blocking probability and total call blocking probability in the central 9 cells and all 49 cells. The simulation results illustrate that the channel borrowing and re-assigning strategy can significantly improve the handoff blocking probability so that the proposed scheme can provide improved mobile services.

Chapter 6 Conclusion

In this thesis, a new DCA scheme with channel borrowing and re-assigning strategy was proposed and its performance was studied through computer simulations in terms of blocking probabilities and handoff activities. The proposed DCA scheme consists of three phases: channel allocation, channel de-allocation, and channel borrowing and re-assignment. After the effects of operational parameters for channel allocation and de-allocation cost functions were examined, the two important parameters used in the cost functions were found to be the interfering-cell available channel condition and the resonance condition. With the channel borrowing and re-assigning strategy, a cell with an empty available channel set may borrow a channel from its neighboring cells. For the no handoff case, simulation results show that the proposed scheme gives the lowest average blocking probability in the central 9 cells and all 49 cells for both uniform and non-uniform traffic distributions. Moreover, the addition of the resonance condition and channel borrowing and re-assigning strategy in the proposed scheme may significantly improve the new call blocking probability of the central 9 cells.

Two mobility models were used to examine the performances of the proposed DCA scheme and some existing channel assignment schemes. An approximate method for estimating the total call blocking probability of the FCA scheme was shown to yield results within $\pm 7\%$ of simulation results. With these two mobility models, the proposed DCA scheme was studied in two different MS maximum speeds (60 and 120 km/hr). At both MS maximum speeds, the proposed scheme significantly improves the handoff blocking probability and the dropped call blocking probability so that it can provide better quality mobile services. The proposed scheme always gives the lowest total call blocking probability in the central 9 cells and all 49 cells.

Furthermore, the effect of the MS maximum speed on the call blocking probabilities in different tier cells was studied. The simulation results show that as the MS maximum speed increases, the blocking probabilities for the first and second tier cells are lowered. However, the increase in the MS maximum speed has little effect on the handoff blocking and the total call blocking probability for the third tier cells.

6.1 Future Works

Some of the more important issues that could be examined in further investigations are as follows

- To analyze the performance of the proposed DCA scheme using other mobility models [21].
- To investigate the performance of the proposed DCA scheme in a fading environment.
- To study the performance of the proposed DCA scheme using a power control algorithm.
- To analyze the performance of the proposed DCA scheme using adaptive channel allocation reuse partitioning schemes [22, 23].

Glossary

A	Area of the circular-shaped cell
$A(x)$	Used channel set of cell x
$B(x)$	A subset of $I(x)$ where cell $y \in B(x)$ has a non-empty available channel set
BCO	Borrowing with Channel Ordering
BDCL	Borrowing with Directional Channel Locking
BS	Base Station
CIR	Carrier-to-Interference Ratio
CIRF	Co-channel Interference Reduction Factor
CP-DCA	Compact Pattern Based Dynamic Channel Assignment
D	The distance between the two nearest co-channel cell centers
$D(x)$	A subset of $I(x)$ where channel i is used in cell $y \in D(x)$
DCA	Dynamic Channel Assignment
FCA	Fixed Channel Assignment
$F_D(x)$	Nominal channel set of cell x
$I(x)$	Interfering cells of cell x
L	Perimeter length of the circular-shaped cell
$L(x)$	A set of co-channel cells separated by the minimum reuse distance D
$\Lambda(x)$	Available channel set of cell x
MS	Mobile Station
MSC	Mobile Switching Center
N	Frequency reuse factor
N_C	Average number of the neighboring cells per cell
p.d.f.	Probability density function
P_b	Total call blocking probability
P_b'	Blocking probability of call channel requests (i.e., new call arrival or handoff arrival)
P_{bh}	Handoff blocking probability

P_{bn}	New call blocking probability
P_{dc}	Dropped call probability
PSTN	Public Switched Telephone Network
R	Cell radius
SB	Simple Borrowing
V	MS speed
V_{\max}	MS maximum speed

Bibliography

- [1] W. C. Y. Lee, *Mobile Cellular Telecommunications Analog and Digital Systems*, 2nd Edition, McGraw-Hill, Inc., 1995.
- [2] T. S. Rappaport, *Wireless Communications Principles and Practice*, Prentice-Hall, Inc., 1996.
- [3] W. C. Y. Lee, *Mobile Communications Design Fundamentals*, 2nd Edition, John Wiley & Sons, Inc., 1993.
- [4] I. Katzela and M. Naghshineh, "Channel Assignment Schemes for Cellular Mobile Telecommunication Systems: A Comprehensive Survey," *IEEE Pers. Comm.*, pp. 10-31, Jun. 1996.
- [5] J. S. Engel and M. M. Peritsky, "Statistically-Optimum Dynamic Server Assignment in Systems with Interfering Servers," *IEEE Trans. Veh. Technol.*, vol. VT-22, no. 4, pp. 203-209, Nov. 1973.
- [6] S. M. Elnoubi, R. Singh, and C. Gupta, "A New Frequency Channel Assignment Algorithm in High Capacity Mobile Communication Systems," *IEEE Trans. Veh. Technol.*, vol. VT-31, no. 3, pp. 125-131, Aug. 1982.
- [7] M. Zhang and T. S. P. Yum, "Comparisons of Channel-Assignment Strategies in Cellular Mobile Telephone Systems," *IEEE Trans. Veh. Technol.*, vol. VT-38, no. 4, pp. 211-215, Nov. 1989.
- [8] K. L. Yeung and T. S. P. Yum, "Compact Pattern Based Dynamic Channel Assignment for Cellular Mobile Systems," *IEEE Trans. Veh. Technol.*, vol. VT-43, no. 4, pp. 892-896, Nov. 1994.
- [9] M. Zhang and T. S. P. Yum, "The Nonuniform Compact Pattern Allocation Algorithm for Cellular Mobile Systems," *IEEE Trans. Veh. Technol.*, vol. VT-40, no. 2, pp. 387-391, May 1991.
- [10] E. Del Re, R. Fantacci, and G. Giambene, "Handover and Dynamic Channel Allocation Techniques in Mobile Cellular Networks," *IEEE Trans. Veh. Technol.*, vol. VT-44, no. 2, pp. 229-237, May 1995.

- [11] L. Ortigoza-Guerrero and D. Lara-Rodriguez, "CPMCB: A Suitable DCA Scheme for the Pan-European GSM System," *Proc. 47th IEEE VTC*, Phoenix, Arizona, pp. 1679-1683, May 4-7, 1997.
- [12] A. Hac and C. Mo, "Dynamic Channel Assignment Strategy for Microcell Systems," *Proc. of IEEE Pacific Rim Conf. on Communication, Computer and Signal Processing*, Victoria, B.C., Canada, Vol. 1, pp. 346-349, Aug. 20-22, 1997.
- [13] J. J. Hopfield and D. W. Tank, "Neural Computation of Decisions in Optimization Problems," *Biological Cybernetics*, vol. 52, pp. 141-152, 1982.
- [14] D. Kunz, "Channel Assignment for Cellular Radio Using Neural Networks," *IEEE Trans. Veh. Technol.*, vol. VT-40, no. 1, pp. 188-193, Feb. 1991.
- [15] E. Del Re, R. Fantacci, and L. Ronga, "A Dynamic Channel Allocation Technique Based on Hopfield Neural Networks," *IEEE Trans. Veh. Technol.*, vol. VT-45, no. 1, pp. 26-31, Feb. 1996.
- [16] K. N. Chang, J. T. Kim, C. S. Yim, and S. Kim, "An Efficient Borrowing Channel Assignment Scheme for Cellular Mobile Systems," *IEEE Trans. Veh. Technol.*, vol. VT-47, no. 2, pp. 602-608, May 1998.
- [17] R. Thomas, H. Gilbert, and G. Mazziotto, "Influence of the Movement of the Mobile Station on the Performance of a Radio Cellular Network," *Proc. 3rd Nordic Seminar*, Paper 9.4, Copenhagen, Sep. 1988.
- [18] D. Hong and S. S. Rappaport, "Traffic Model and Performance Analysis for Cellular Mobile Radio Telephone Systems with Prioritized and Nonprioritized Handoff Procedures," *IEEE Trans. Veh. Technol.*, vol. VT-35, no. 3, pp. 77-92, Aug. 1986.
- [19] H. Xie and S. Kuek, "Priority Handoff Analysis," *Proc. 43rd IEEE VTC*, Secaucus, New Jersey, pp. 855-858, May 18-20, 1993.
- [20] H. Xie and D. J. Goodman, "Mobility Models and Biased Sampling Problem," *Proc. of 2nd IEEE International Conference on Universal Personal Communications*, Ottawa, Ontario, pp. 803-807, Oct. 12-15, 1993.
- [21] K. Lam, *Location Updating and Paging Strategies in a Cellular System*, M.A.Sc. Thesis, The University of British Columbia, Apr. 1993.

- [22] T. Takenaka, T. Nakamura, and Y. Tajima, "All-Channel Concentric Allocation in Cellular Systems," *IEEE ICC*, pp. 920-924, 1993.
- [23] H. Furukawa and Y. Akaiwa, "Self Organized Reuse Partitioning, a Dynamic Channel Assignment Method in Cellular System," *Proc. 43rd IEEE VTC*, Secaucus, New Jersey, pp. 524-527, May 18-20, 1993.